AWARD NUMBER: W81XWH-15-1-0196

TITLE: Engineering Irisin for Understanding Its Benefits to Obesity

PRINCIPAL INVESTIGATOR: Yousong Ding

CONTRACTING ORGANIZATION: University of Florida
Verobeach, FL 32962

REPORT DATE: March 2018

TYPE OF REPORT: Final

PREPARED FOR: U.S. Army Medical Research and Materiel Command
Fort Detrick, Maryland 21702-5012

REPORT DOCUMENTATION PAGE

Form Approved
OMB No. 0704-0188

1. REPORT DATE	2. REPORT TYPE	3. DATES COVERED
March 2018	Final	07/01/2015 to 12/31/2017

4. TITLE AND SUBTITLE
Engineering Irisin for Understanding Its Benefits to Obesity

5a. CONTRACT NUMBER

5b. GRANT NUMBER
W81XWH-15-1-0196

5c. PROGRAM ELEMENT NUMBER

6. AUTHOR(S)
Yousong Ding

E-Mail: yding@cop.ufl.edu

5d. PROJECT NUMBER

5e. TASK NUMBER

5f. WORK UNIT NUMBER

7. PERFORMING ORGANIZATION NAME(S) AND ADDRESS(ES)
University of Florida 207 Grinter Hall, Gainesville, FL 32611

8. PERFORMING ORGANIZATION REPORT NUMBER

9. SPONSORING / MONITORING AGENCY NAME(S) AND ADDRESS(ES)

U.S. Army Medical Research and Materiel Command
Fort Detrick, Maryland 21702-5012

10. SPONSOR/MONITOR'S ACRONYM(S)

11. SPONSOR/MONITOR'S REPORT NUMBER(S)

12. DISTRIBUTION / AVAILABILITY STATEMENT

Approved for Public Release; Distribution Unlimited

13. SUPPLEMENTARY NOTES

14. ABSTRACT

Irisin is an exercise-induced myokine and has initially showed a promising function in browning white adipose tissue and increasing energy expenditure. The overall objective of the proposed project is to engineer irisin for uncovering its signaling in obesity, with the ultimate hope to capture its benefits for obesity prevention and treatment. The hypothesis is that physiological and pharmacological functions of irisin can be interpreted and controlled through identifying and targeting irisin receptor (IR). Over the last awarding period, we have made several significant discoveries that partially test the hypothesis and achieve the objective. Specifically, we have identified a putative region for irisin-IR interactions and validated the involvement of this region through producing irisin mutants and examining their browning activity in 3T3-L1 adipocytes. We further attempted to use the yeast expression system to produce unnatural aminio acid labelled irisin variants that expectedly capture the interactions between irisin and IR for IR identification. After extensive optimization of conditions in the yeast system, we later switched to the bacterial system and successfully produced such irisin variants. Finally, we used these variants to start the studies to capture IR. These results provided a solid foundation to accomplish proposed work in the next six months.

15. SUBJECT TERMS
Irisin, obesity, irisin receptor, unnatural amino acid, cross-linking, mass spectroscopy.

16. SECURITY CLASSIFICATION OF:			17. LIMITATION OF ABSTRACT	18. NUMBER OF PAGES	19a. NAME OF RESPONSIBLE PERSON
a. REPORT	b. ABSTRACT	c. THIS PAGE			USAMRMC
Unclassified	Unclassified	Unclassified	Unclassified	30	19b. TELEPHONE NUMBER *(include area code)*

Table of Contents

Page

1. Introduction

Obesity is the most common metabolic disorder in the world, and about 13 % of active-duty military personnel were classified as obese in 2008, posing a significant threat to national security. Irisin, an exercise-induced myokine, has initially showed a promising function in browning white adipose tissue and increasing energy expenditure, both critical to fight against obesity and its related diseases. Since then, a number of studies have been directed to evaluate the physiological and pharmacological effects of irisin in adipocytes as well as many other tissues/organs, and to elucidate its signaling pathways. Despite these significant achievements in the irisin research, little is known about the receptor system through which irisin may act. The overall objective of the proposed project is to engineer irisin for uncovering its signaling in obesity, with the ultimate hope to capture its benefits for obesity prevention and treatment. The hypothesis is that physiological and pharmacological functions of irisin can be interpreted and controlled through identifying and targeting irisin receptor (IR). To test the hypothesis and to accomplish the objective, we aim to identify the IR from 3T3-L1-derived adipocytes. A novel *in vivo* genetically incorporating unnatural amino acid (UAA) into proteins for site-specific cross-linking (UAA-SSC) approach will be employed for receptor identification in this project.

2. Keywords

Irisin, irisin receptor (IR), obesity, 3T3-L1, unnatural amino acid (UAA), cross-linking, SDS-PAGE, Western blotting, adhesion GPR, mass spectroscopy, *Pichia pastoris*, *E. coli*, fluorescence, Ucp-1, *p*-benzoyl-L-phenylalanine (pBpa), *p*-azido-L-phenylanaline (pAzpa), aminoacyl-tRNA synthetase/suppressor tRNA (aaRS/tRNA$_{CUA}$), extracellular vesicle (EV), high resolution (HR), fibronectin type III domain containing 5 (FNDC5).

3. Accomplishments

3.1. What were the major goals of the project?

Major Goals	Timeline
Major Task 1 : Generation of UAA labeled irisin	Months
Subtask 1.1: Prepare yeast expression system and create irisin mutants:	July 1st to Sept. 30th, 2015
Subtask 1.2: Produce irisin variants carrying pBpa and pAzpa in small scale:	Oct. 1st to Dec. 31st, 2015
Subtask 1.3: Produce irisin variants carrying pBpa and pAzpa in a large volume:	Jan. 1st to June 30th, 2016
Subtask 2: Verify pBpa and pAzpa incorporation into irisin	Nov. 1st, 2015 to June 30th, 2016
Subtask 3: Verify activity of UAA labeled irisin variants	Apr. 1st to Sept 30th, 2016
Milestone(s) Achieved: production and purification of a number of active UAA labeled irisin variants.	9-15 months
Major Task 2: Identification of irisin receptor	
Subtask 1: Generate cross-linked products	Apr. 1st to Sept 30th, 2016
Subtask 2: Identify irisin receptor	Aug 1st to Dec 31st, 2016

3.2. What was accomplished under these goals?

For the entire award period, our major activities included the generation of additional UAA labeled irisin variants, and the isolation and identification of IR. Our specific objectives were to produce UAA-labeled irisin variants and then test their activities in browning differentiated 3T3-L1 adipocytes, isolate IR by crossing-linking studies and identify IR by proteomics approach. The major findings/outcomes of our studies over the entire award period included (1) the validation of a promising site for irisin-IR interaction, (2) the successful generation of seven UAA-labeled irisin variants in *E. coli*, (3) the impaired browning activity of UAA-labeled irisin variants and other types of variants, and (4) the identification of IR though UAA-SSC approach. Despite multiple efforts and significant research progresses made over the entire award period, we unfortunately failed in isolating and identifying IR. On the other hand, a recent publication (***Science Translational Medicine***, 2017, 9 (418):eaao6298) provides compelling results indicating that irisin may mediate its beneficial effects through interacting with IR ***inside*** cells. Details about our studies, results and discussions are shown below.

A. Prepare UAA-labeled irisin variants.

A1. Produced recombinant His tagged irisin. *Pichia pastoris* X-33 is a feasible system to produce a large quantity of recombinant wild type irisin (r-irisin) for the investigation of bioactivity and signaling. To facilitate the protein purification and enrichment, a 6xHis-tag was added on the 3'-end of codon-optimized *irisin* cDNA through a PCR reaction. The amplicons were cloned into pPICZαA vector for expressing r-irisin-His in *P. pastoris* X-33 cells. A single colony was picked from plates and grown in 10 mL of YPD medium overnight. The overnight culture was then transferred to 500 mL of YPD medium and grown to be near saturation. Cultures were centrifuged and the cell pellets were then resuspended in 150 mL of BMMY (100 mM potassium phosphate, pH 6.0, 1.34% YNB, 4×10^{-5} biotin, and 0.5% methanol) for induction. After 6 days of growth (30 °C, 250 rpm, with 0.5% methanol and volume supplementation), the supernatant was harvested after centrifugation and adjusted to pH 7.4 for protein purification with Ni-NTA affinity chromatography. The purified r-irisin-His protein was separated as three bands (MW = 27, 24, and 17 kDa) reflecting the different glycosylation status in SDS-PAGE analysis (**Fig. 1**). This pattern was the same as the r-irisin. The His-tag adds about 2 kDa to the MWs of r-irisin-His.

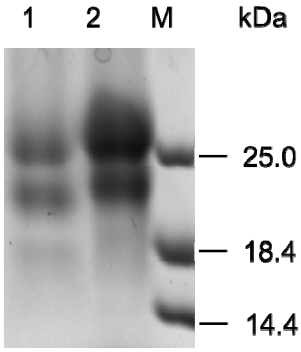

Fig. 1. Expression of r-irisin protein in *Pichia pastoris* X-33. Lane 1: wild type r-irisin; lane 2: r-irisin with a C-His tag (r-irisin-His).

A2. Probing irisin-IR interactions. After examining irisin crystal structure, we identified a region comprising three flexible structural elements, N-terminus 1-5 (SPSAP) and two loops with residues 55–58 (EDEV) and residues 106–108 (SIQ) as a promising site for irisin's interactions with IR (**Fig. 2A**). To probe the involvement of this region, we mutated each of 11 non-alanine residues in this region to alanine, and successful expressed eight (except P5A, E55A, and S106A) in *P. pastoris* as described above (**Fig. 2B**). We next characterized six r-irisin alanine

variants in inducing the overexpression of *Ucp-1* mRNA in differentiated 3T3-L1 adipocytes by quantitative reverse transcription polymerase chain reaction (RT-qPCR) (**Fig. 2C**). Briefly, 3T3-L1 preadipocytes were cultured using basic DMEM medium at 37°C in a 5% CO_2 incubator. After confluence (day 1), the cells were initiated for the adipocyte differentiation by incubating with induction medium. On day 3, r-irisin and r-irisin alanine variants as well as two negative controls (yeast supernatant and PBS) were added to the 3T3-L1 cells for a total of 4-day stimulation. On day 7, treated 3T3-L1 mature adipocytes were processed for RNA extraction and then RT-qPCR for quantitating the levels of *Ucp-1* mRNA. Ucp-1 is an established biomarker of browning white adipocytes and is commonly used to evaluate the browning activities of irisin. All alanine variants (except D56A) exhibited significantly reduced activity (two to four folds), compared to r-irisin, and the activity of r-irisin E57A was even diminished to the same levels of two negative controls. Furthermore, the binding abilities of these alanine variants to differentiated 3T3-L1 adipocytes were evaluated by flow cytometry (**Fig. 1D**). 3T3-L1 cells were released by trypsin and incubated with r-irisin and r-irisin alanine variants for 60 min at room temperature. The cells were then washed and resuspended in PBS/0.5% BSA. Fifty thousand events per sample were acquired using a FACS Calibur flow cytometer (BD Bioscience, San Jose, CA). Interestingly, this analysis indicated that the majority of alanine variants (P2A, D56A, V58A, I107A and Q108A) retain the similar binding ability to wild type r-irisin, while r-irisin E57A even shows the increased binding ability (1.2-fold). These results demonstrated the importance of the selected regions in irisin's signaling, but on the other hand, indicated that the binding of irisin-IR might be determined by other factors, but not single site of selected regions.

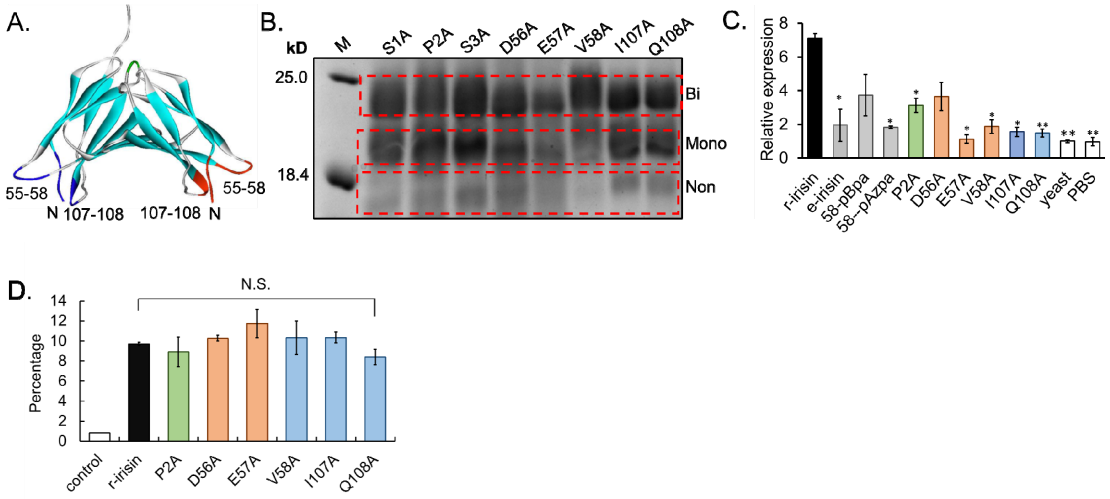

Fig. 2. A: Dimeric irisin crystal structure (PDB: 4LSD) contains one region per monomer, which comprises the N-terminus and two loops and may participate in irisin-IR binding. **B:** SDS-PAGE analysis of eight r-irisin alanine mutants expressed in *P. pastoris*. **C:** Upregulation of *Ucp-1* mRNA levels in differentiated 3T3-L1 adipocytes by a variety of irisin analogs. **D**: Binding of r-irisin and alanine variants to differentiated 3T3-L1 adipocytes. Yeast supernatant was used as negative control. All experiments were repeated multiple times (n > 3). Results are presented as mean ± S.E. and compared by one-way ANOVA between r-irisin group and other groups. The means were considered statistically different when the probability of the event was determined to be below 5% (P <0.05). *P<0.05, **P<0.01.

A3. Introducing amber stop codons to the selected sites of irisin. For genetic incorporation of unnatural amino acid (UAA) into any protein, the orthogonal aminoacyl-tRNA synthetase/suppressor tRNA (aaRS/$tRNA_{CUA}$) pairs are required. Since the amber codon (UAG) is rarely recognized by the endogenous host tRNAs, tRNA charging with UAA and the relevant

aaRS were engineered to recognize this codon. In our studies, the amber codon was successfully engineered into irisin by PCR technology using pPICZα-irisin-C-His as the template. Sequencing results clearly showed that all 12 sites of the selected region (**Fig. 2A**) were mutated to amber stop codons in irisin mutants (**Fig. 3**).

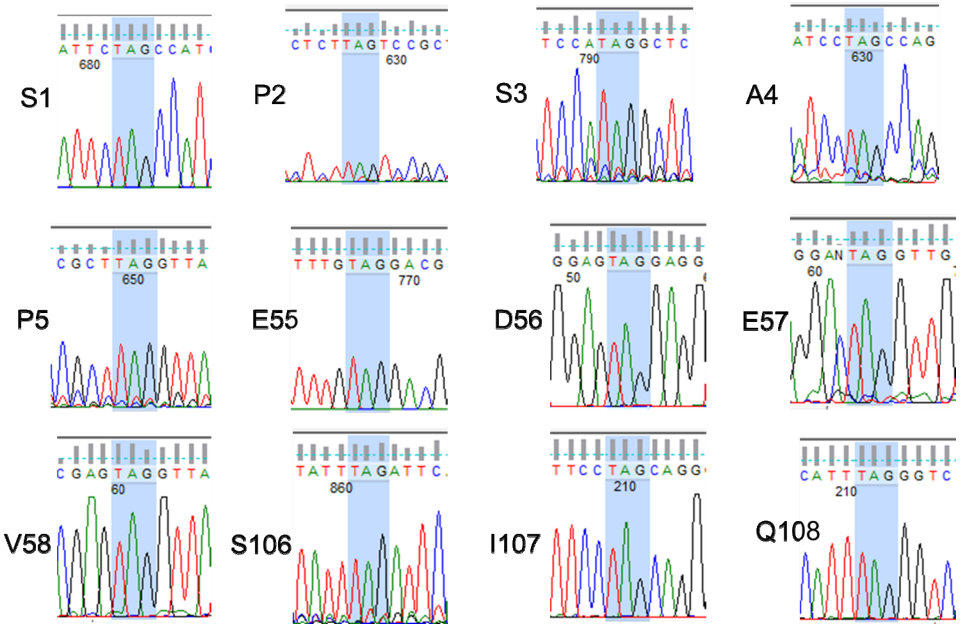

Fig. 3. Sequencing results revealed the amber codon in 12 engineered irisin mutants.

A4. Engineered P. pastoris *system with two orthogonal aaRS/tRNA$_{CUA}$ pairs*. The Schultz laboratory (Scripps) has developed pREAV-P$_{FLD1}$-pBpa and pREAV-P$_{FLD1}$-pAzpa plasmids that incorporate photoactive *p*-benzoyl-L-phenylalanine (pBpa) and *p*-azido-L-phenylanaline (pAzpa) in proteins when expressed in *P. pastoris* GS200. Following the protocols developed in his laboratory, we made competent cells of *P. pastoris* GS200 for transformation. To create GS200/pREAV-P$_{FLD1}$-pBpa, 200 ng of *Aat*II linearized pREAV-P$_{FLD1}$-pBpa and pREAV-P$_{FLD1}$-pAzpa (obtained from the Schultz laboratory) were electroporated into *P. pastoris* GS200 competent cells. To confirm the proper incorporation of aaRS/tRNA$_{CUA}$ genes into yeast chromosome, PCR reactions were performed to detect the integration of pREAV plasmids using the genomic DNAs (gDNA) of engineered yeast cells as the templates. The identification of PCR products at around 800 bp confirmed the integration of pREAV-P$_{FLD1}$-pBpa and pREAV-P$_{FLD1}$-pAzpa in *P. pastoris* GS200, respectively (**Fig. 4A**).

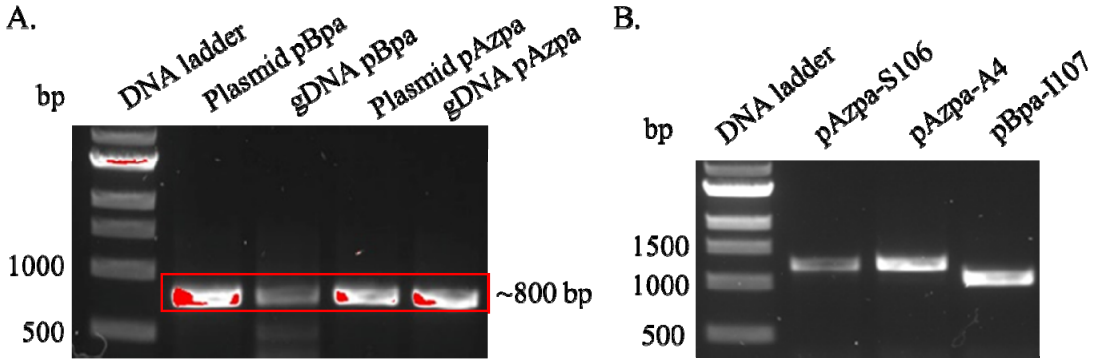

Fig. 4. A: Amplification of aaRS/tRNA$_{CUA}$ genes from the genomic DNAs of engineered *P. pastoris* GS200 cells carrying pREAV-P$_{FLD1}$-pBpa and pREAV-P$_{FLD1}$-pAzpa. **B:** PCR analysis confirmed the incorporation of three irisin mutant genes with the amber codon in *P. pastoris* GS200/pREAV-P$_{FLD1}$-pBpa or *P. pastoris* GS200/pREAV-P$_{FLD1}$-pAzpa cells.

A5. Expressed UAA-labeled r-irisin variants in P. pastoris *GS200.* To express UAA-labeled r-irisin variants, all 12 constructs carrying irisin genes mutated with the amber codon were transformed into *P. pastoris* GS200/pREAV-P_{FLD1}-pBpa and *P. pastoris* GS200/pREAV-P_{FLD1}-pAzpa competent cells. pPICZα-irisin-C-His and pPICZα-irisin were used as two controls. Colonies of *P. pastoris* GS200-$irisin_{S106}$/pREAV-P_{FLD1}-pAzpa, *P. pastoris* GS200-$irisin_{A4}$/pREAV-P_{FLD1}-pAzpa and *P. pastoris* GS200-$irisin_{I107}$/pREAV-P_{FLD1}-pBpa were randomly picked for PCR analysis. The results confirmed the successful integration of irisin mutant genes into the yeast chromosome (**Fig. 4B**). Next, we attempted to express several UAA-labeled r-irisin variants in small scale. Colonies of *P. pastoris* GS200-$irisin_{TAG}$/pREAV-P_{FLD1}-pBpa and *P. pastoris* GS200-$irisin_{TAG}$/pREAV-P_{FLD1}-pAzpa were picked from plates and grown to near saturation (OD_{600}≈12-18) in 10 mL of YPD medium. After centrifugation and washing, the cell pellets were then resuspended in 2 mL of Buffered Minimal Methanol Histidine (BMMH) with 2 mM pBpa or pAzpa. Protein expression was continuously induced with methanol supplementation to 0.5% every 24 h. Media (200 μL, 10% culture volume) or sterile water was added every 24 h to account for evaporation. After three days, clear supernatant was collected from media (50 μL) after centrifugation. We then detected the recombinant UAA-labeled r-irisin variants in the clear supernatant by SDS-PAGE and Western blotting analysis using home-made high quality rabbit anti-irisin antibody. R-irisin showed three bands at the expected positions in both SDS-PAGE and western blotting (**Fig. 5**). These results indicated that the *P. pastoris* GS200 system is capable to produce recombinant r-irisin. However, we did not detect the production of any UAA-labeled r-irisin variants, r-irisinA4pAzpa, r-irisinE55pAzpa, r-irisinE57pAzpa, r-irisinE57pBpa, r-irisinV58pAzpa, and r-irisinS106pAzpa, in this work. Furthermore, we expressed these variants in the large scale (150 mL of BMMH) for six days, but observed no production of any variant. We then attempted to optimize a variety of culturing conditions. The same results were observed after optimizing shaking speed, induction temperature, expression time, UAA concentrations, and inoculation volumes. We also expressed multiple colonies generated from the same transformation. Furthermore, we expressed additional irisin mutant genes in both *P. pastoris* GS200/pREAV-P_{FLD1}-pBpa and *P. pastoris* GS200/pREAV-P_{FLD1}-pAzpa. However, none of these efforts led to any expression of UAA-labeled irisin variants. Finally, both pBpa and pAzpa showed expected molecular weights in mass spectroscopy (MS) analysis. It remains unclear about the causes of failed expression of UAA-labeled r-irisin in the *P. pastoris* GS200 system.

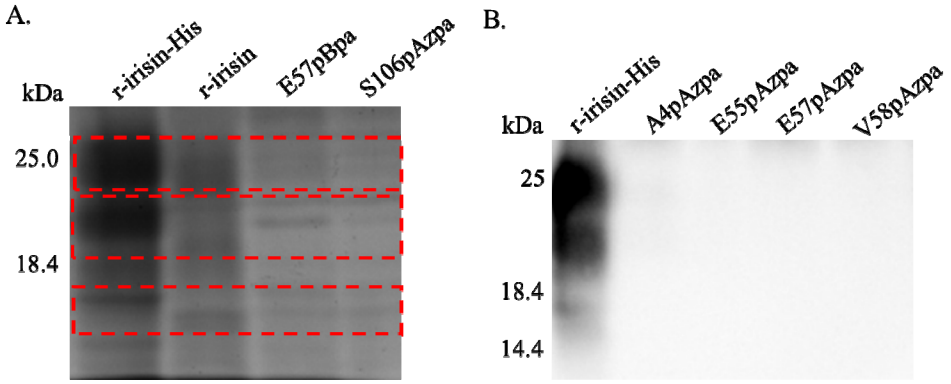

Fig. 5. A: SDS-PAGE analysis of r-irisin-His, r-irisin, r-irisinE57pBpa, and r-irisinS106pAzpa expressed in *P. pastoris* GS200 engineered with pREAV-P_{FLD1}-pBpa or pREAV-P_{FLD1}-pAzpa. Only two wild type r-irisin were successfully produced. **B:** Western blotting analysis of r-irisin-His, r-irisinA4pAzpa, r-irisinE55pAzpa, r-irisinE57pAzpa, and r-irisinV58pAzpa in *P. pastoris* GS200 engineered with pREAV-P_{FLD1}-pAzpa. None of pAzpa-labeled r-irisin variants were produced to the detectable level.

A6. Expressed UAA-labeled irisin variants in E. coli. Since the *P. pastoris* expression system met the unknown/unexpected challenge in producing UAA-labeled irisin variants, we turned our efforts to prepare these variants in the *E. coli* system. *E. coli* has been used as the host to prepare irisin for crystallization studies. We reason that if UAA-labeled irisin variants from the *E. coli* system retain the browning activity, they should serve the same function in capturing IR. In fact, recombinant irisin produced in *E. coli* (e-irisin) has been commercially available and used in a number of biomedical publications, although *E. coli* has no ability to catalyze post-glycosylation modifications, thereby producing only nonglycosylated irisin. Furthermore, compared with the *P. pastoris* system, *E. coli* is most commonly used to produce UAA-labeled proteins in large quantities. To validate the feasibility of *E. coli* system, we expressed the irisin gene and purified a large quantity of e-irisin (**Fig. 6A**). We observed that the activity of e-irisin in upregulating the expression of *Ucp-1* mRNA was less than r-irisin but significantly higher than two negative controls (yeast control and PBS) in qRT-PCR analysis (**Fig. 2C**). This result clearly indicated that the *E. coli* expression system can be an alternative to the *P. pastoris* expression system in producing **active** irisin. To examine the production of UAA-labeled e-irisin, we first introduced the amber codon to the V58 site of irisin gene and cloned the resultant into the expression vector pET26. The construct was then co-transformed into *E. coli* BL21 (DE3) with pEVOL-pBpa or pEVOL-pAzpa encoding an orthogonal aaRS/tRNA$_{CUA}$ pair specific to pBpa or pAzpa (obtained from Addgene), respectively. A single colony from each cotransformation was picked up to produce UAA-labeled e-irisin in 2xYT medium containing 1 mM UAA upon inductions with arabinose and IPTG. The expressed proteins were purified by the Ni-NTA affinity chromatography through the C-terminal His-tag. Both e-irisinV58pAZpa and e-irisinV58pBpa were undoubtedly detected as the single band in SDS-PAGE analysis, whose intensity increased with protein concentration (**Fig. 6A**). These bands correspond to the nonglycosylated irisins, the same as WT e-irisin. The proper incorporation of pBpa in nonglycosylated e-irisin variant was further confirmed by its molecular weight by MALDI-TOF mass spectrometry analysis (**Fig. 6B**). MW of WT e-irisin was 13426.2 (detected MW: 13421.31, data not shown). Remarkably, we observed that e-irisinV58pBpa showed higher activity in upregulating *Ucp-1* expression than e-irisin while the activity of e-irisinV58pAZpa was the same as WT in qRT-PCR analysis (**Fig. 2C**). These results demonstrated the viable *E. coli*-based approach to produce active UAA-labeled irisin variants and provided supportive evidence to the involvement of the loop55-58 in irisin-IR interactions.

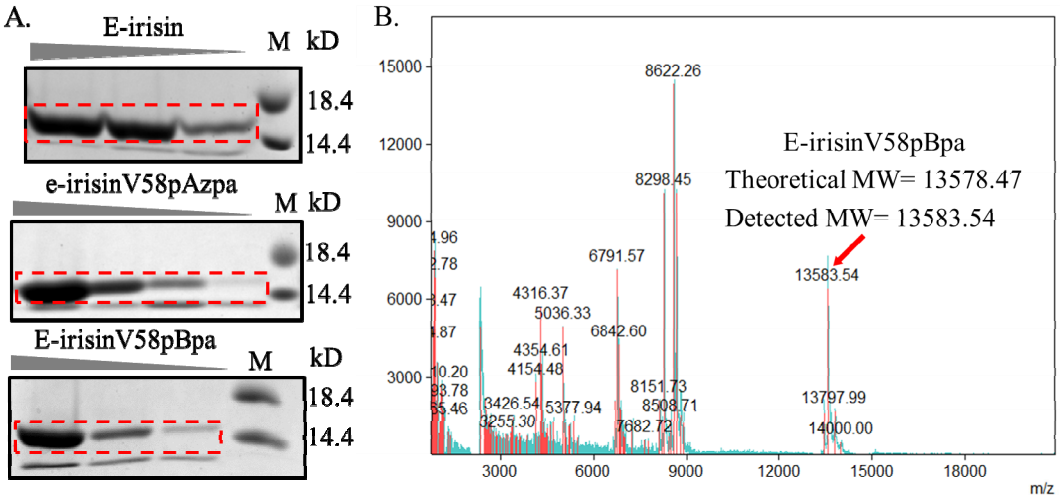

Fig. 6. A: SDS-PAGE analysis of recombinant WT e-irisin and two UAA labeled e-irisin variants expressed in *E. coli* BL21 (DE3). **B:** MOLDI-TOF MS spectrum of e-irisinV58pBpa to confirm the proper incorporation of pBpa at V58 of e-irisin. The observed MW difference (~5 aum) was in the normal range of instrument error.

After the encouraging success of proof-of-concept studies, we followed the same protocol to produce additional 22 UAA-labeled e-irisin. The amber codon was introduced to the selected sites (S1, P2, S3, A4, P5, E55, D56, E57, V58, S106, I107 and Q108) of irisin gene and cloned into the expression vector pET26. Next, irisin$_{TAG}$-pET26b constructs were co-transformed with pEVOL-pBpF or pEVOL-pAzpa plasmid into *E. coli* BL21 (DE3). pBpa or pAzpa-labelled irisin proteins were expressed in the presence of 1 mM pBpa or pAzpa. The SDS-PAGE analysis revealed the successful expression of soluble e-irisinS1pAzpa, e-irisinP2pAzpa, e-irisinS1pBpa, e-irisinP2pBpa and e-irisinA4pBpa (**Fig. 7A-B**). The expressed proteins were then purified by Ni-NTA resin. They were further analyzed by high resolution (HR) electrospray LC-MS analysis and showed the expected molecular weights, thus verifying the incorporation of UAAs in purified e-irisin variants (**Fig. 7C**). However, all other 17 variants were either insoluble or not expressed after a variety of efforts such as varying culturing and induction conditions. For example, e-irisinA4pBpa is successfully expressed but its counterpart e-irisinA4Azpa is not available, likely indicating potential effects of Azpa on the protein folding.

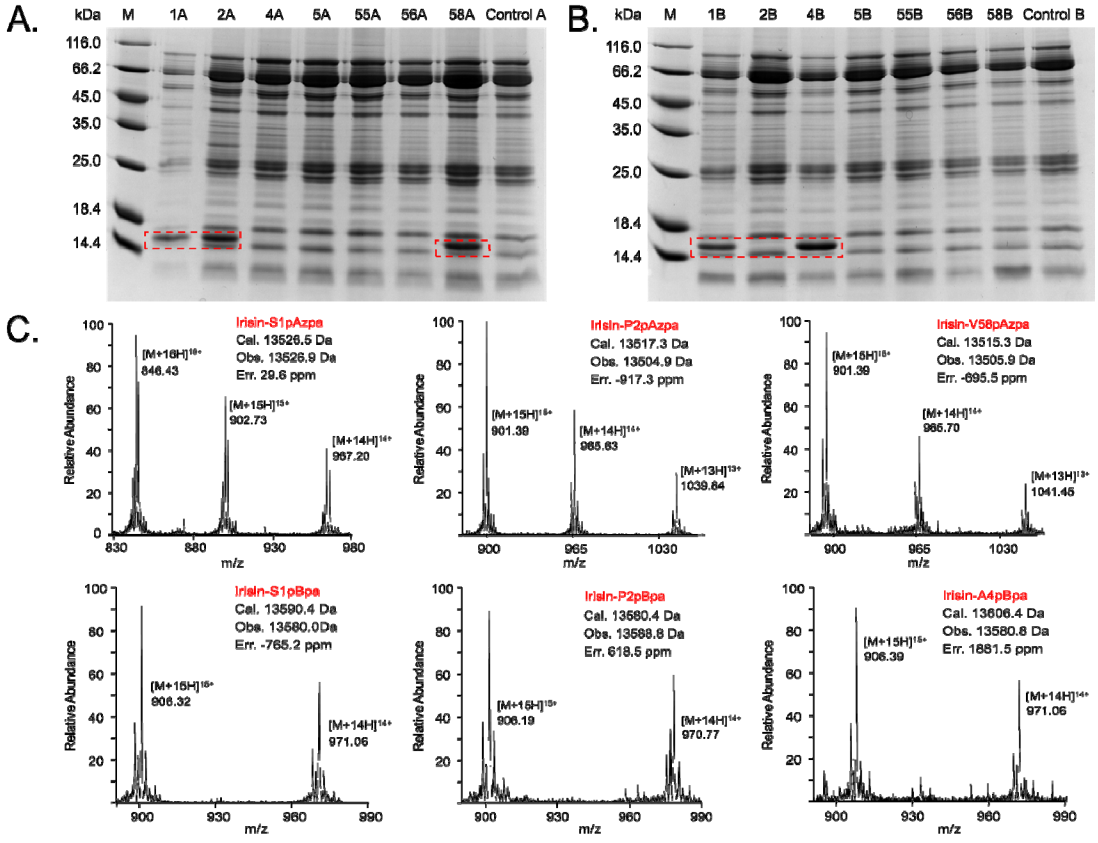

Fig. 7. A: SDS-PAGE analysis of UAA labeled e-irisin variants expressed in *E. coli* BL21 (DE3). pAzpa and pBpa are abbreviated as A and B, respectively. **B:** HR-MS spectra of UAA labeled e-irisin variants confirm the proper incorporation of pAzpa or pBpa.

B. Identification of irisin receptor (IR).

B1. Binding of r-irisin to differentiated 3T3-L1 cells. We have visualized irisin binding to cell surfaces by detecting luciferase signals and its C-terminal His-tag in two recent publications (*Diabetes*. 2014, 63:514-25; *PLoS One*. 2015, 10:e0136816). To further quantitate irisin binding, we labeled r-irisin with a fluorescent probe, fluorescein isothiocyanate (FITC), following the maufacture protocol (Thermo Scientific). We then incubated FITC-irisin with differentiated 3T3-

L1 cells, followed by centrifugation and washing to remove unbound materials. In fluorescence imaging study, FITC-irisin was clearly enriched on cell surface while FITC itself showed minimal signal (**Fig. 8A**). Furthermore, the fluorescence signal increased with the concentration of FITC-irisin (up to 25 μg/mL) (**Fig. 8B**). This result further confirmed the existence of IR and preliminarily characterized the binding capacity of differentiated 3T3-L1 adipocytes.

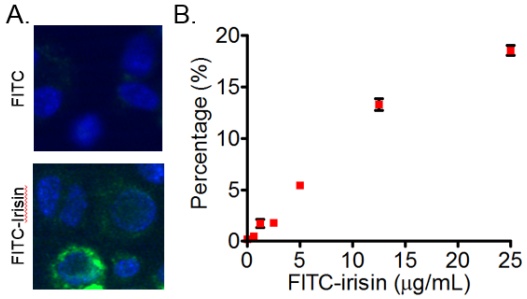

Fig. 8. A: Fluorescence imaging of 3T3-L1 adipocytes with FITC (top) and FITC-irisin (bottom). Irisin showed specific binding to 3T3-L1 cell surface. **B:** The FITC-irisin binding to 3T3-L1 was dose dependent.

B2. Generated cross-linked products. The availability of multiple UAA-labeled e-irisin variants with large quantities allowed the crosslinking studies to isolate the potential IR. Differentiated 3T3-L1 cells were detached by trypsin treatment and then transferred to the petri dishes. The cell suspension was then incubated with UAA-labeled e-irisins at room temperature for 1 h. To maximize the success rate, e-irisin variants with UAA incorporation at *N*-terminal region 1-5 (SPSAP) and loop region 55–58 (EDEV) were combined in crosslinking experiments. After the incubation, the culture was irradiated at 365 nm with a hand-held UV lamp (11 V, 60 Hz, 0.2 A) at the distance of 2.5 cm on ice for 30 min. The cells were harvested, washed, and then lysed with Pierce IP lysis buffer (Thermo Fisher Scientific). The cell lysis (crosslinking products) and cell wash supernatant (unbound e-irisin variants) were analyzed by western blotting using home-made high quality anti-irisin antibody. Differentiated 3T3-L1 cells without e-irisin treatment were used as negative controls. Unfortunately, the crosslinking experiments failed to reveal any new bands that are not present in controls or supernatant (**Fig. 9**). This result might suggest (1) the abundance of IR on 3T3-L1 cells is extremely low; (2) the protocols for photo crosslinking and membrane protein isolation might not be fully developed; or (3) irisin might not initiate its signaling through interacting on any receptor on cell membrane.

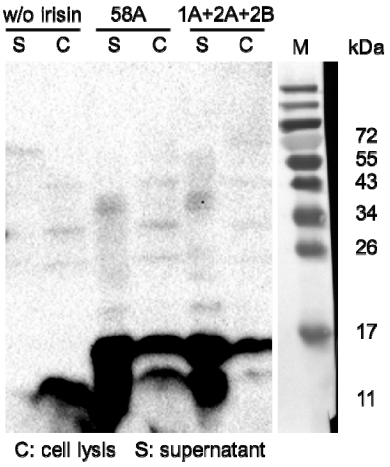

Fig. 9. Western blotting analysis of samples prepared from differentiated 3T3-L1 cells crosslinked with UAA-labelled e-irisin variants.

3.3. What opportunities for training and professional development has the project provided?

Nothing to report.

3.4. How were the results disseminated to communities of interest?

Over the entire award period, the promising results were disseminated to scientific communities multiple times. On Nov 11th, 2015, some results were disseminated in a seminar by the PI to over 200 freshmen at the University of Florida in Sciences for Life program. Some results were further disseminated in seminar to about 50 students in the UF Chemistry Club affiliated with American Chemical Society on Feb 4th, 2016 and Jan 26th, 2017, some results were disseminated in a seminar by the PI to about 50 students in the UF. Furthermore, the PI was invited to deliver a seminar entitled "Beneficial Effects of Irisin on Human Health" in the Annual Meeting of American Chemical Society Florida Section (May 5th to 7th, 2016). In addition, Prof. Li-jun Yang included some results in a seminar organized by the veterinary medical school at Louisiana State University in September, 2016. These outreach activities to local communities at the University of Florida very likely enhanced public understanding of obesity and new treatment options, and increased interest of next-generation scientists in learning and careers in science, technology, and the humanities. At last, some results of this projects were included in a publication coauthored by the PI and Co-PI (Prof. Li-jun Yang) (Irisin exerts dual effects on browning and adipogenesis of human white adipocytes. *Am J Physiol Endocrinol Metab.* 2016 Aug 1;311(2):E530-41).

3.5. What do you plan to do during the next reporting period to accomplish the goals?

This project was officially ended on Dec 31st, 2017.

4. Impact

4.1. What was the impact on the development of the principal discipline(s) of the project?

Obesity is a common, serious, and costly disorder affecting over 1/3 adults in the USA, and its prevalence and high health and economic burdens has also become a serious threat to national security. Previously, a novel exercise-induced hormone has shown an attractive function to induce the loss of body weight, marking it as a promising molecule to fight obesity. In this project, we already engineered and produced several hormone homologs and assessed their bioactivities. These results laid a solid foundation for uncovering the fundamental basis of hormone's functions, thereby providing new promising opportunities to better capture its anti-obesity benefits.

4.2. What was the impact on other disciplines?

This project focused on genetic engineering a novel hormone with chemically defined amino acids that are not available in nature to investigate the underlying principles of its therapeutically relevant activities. The successful completeness of this project, which has been partially achieved during the past awarding period, will indicate that the primary approach used in this work is likely to be generally applicable in the investigations of a number of existing and new biomolecules. Such biomolecules are increasingly available along with the exponential growth of omics data and the advances of other principles (e.g., systems biology and synthetic biology).

4.3. What was the impact on technology transfer?

Nothing to report.

4.4. What was the impact on society beyond science and technology??

This project aims to answer a fundamental question, how an exercise-induced hormone exerts its anti-obesity functions. The results of this project very likely improve public knowledge and attitudes to physical activities, encourage more people to participate in exercise. These changes can consequently enhance public health, increase military readiness, and reduce the overall cost of health system.

5. Changes/problems

5.1. Changes in approach and reasons for change.

During the first year of this award, we sought to express unnatural amino acid (UAA)-labeled irisin variants using *Pichia pastoris* system. The capability of this system has been demonstrated by the successful production of human serum albumin variants carrying different UAAs, as shown in a report from the Prof. Peter Schultz laboratory (Biochemistry, 2009, 48: 2643–2653). In addition, we used the *P. pastoris* system to produce recombinant wild type irisin in the gram scale. However, for some unknown reasons, none of UAA-labeled irisin variants were expressed with the *P. pastoris* system in both small and large scales of culturing and after optimizing a variety of culturing conditions, as shown in SDS-PAGE and Western Blotting analyses. On the other hand, recombinant wild type irisin (e-irisin) produced with *E. coli* system has been commercially available and used in a number of biomedical publications. In our studies, we also produced e-irisin and further confirmed its browning activity. To identify the irisin receptor (IR), we therefore obtained a plasmid encoding orthogonal suppressor tRNA and amino-acyl tRNA synthetase pairs in *E. coli* and expressed UAA-labeled e-irisin variants using the *E. coli* system. Encouragingly, two variants were successfully expressed to a significant level in the proof-of-concept studies. We further confirmed the UAA incorporation in one variant using MS analysis, and assessed the browning activity of these variants as well. Therefore, we adapted a method different with what was shown in the proposal to produce key experimental materials, UAA-labeled irisin variants, to achieve the overall objective. Such a reasonable and mild change in methodology had minor, if any, effects on research direction and final outcomes and was actually helping advance the proposed studies in a timely manner.

During the second year of the award period, we generated several UAA labeled e-irisin variants and performed cross-linking experiments to isolate IR from differentiated 3T3-L1 cells. However, western blotting analysis revealed no obvious crosslinked bands from whole cell lysate in comparison with the negative control. *These results raise several critical but unanswered questions related to irisin research*, for example, what is the form of irisin (free protein cleaved from fibronectin type III domain containing 5, FNDC5, or intact FNDC5) and is irisin receptor available on cell membrane? In fact, since the discovery of irisin in 2012, many discrepant results of the circulating irisin levels have been reported (Eur J Endocrinol July 14, 2017 EJE-17-0572, doi: 10.1530/EJE-17-0572). Scientific community has suspected that the quality and accuracy limitation of existing commercial enzyme-linked immunosorbent assays (ELISAs) may be causative factor (2015, Sci. Rep. 5, 8889). We observed that r-irisin at 5 μM (significantly higher than its detected concentration of 3 ng/mL in human blood) reaches the saturation binding to 3T3-L1 adipocytes but only less than 20% cells interacted with r-irisin (**Figs. 2D and 8B**). The low binding ability of irisin to 3T3-L1 further casts doubt on the actual format of irisin in human and the existence of IR on cell surface. Supportively, our photo cross-linking experiments failed to isolate any putative IR. Very recently, a paper published in the top journal Science

Translational Medicine (*Sci Transl Med*. 2017 Nov 29; 9(418). pii: eaao6298.) clearly revealed that ***irisin, via lipid raft-mediated endocytosis, enters alveolar cells and targets mitochondria in animal studies***. Although the targeted cells are not 3T3-L1 or other types of adipocytes, the endocytosis of irisin from blood stream into cells can be a conserved mechanism, suggesting that IR, if existing, may be on mitochondria membrane. Indeed, our previous paper demonstrated significant effects of irisin on mitochondria thermogenesis using H9C2 cells as the model (*PLoS One*. 2015 Aug 25;10(8):e0136816.). The results in these multiple papers together suggest that the lack of UAA-irisin-IR after crosslinking might not be surprised.

We further examined the format of irisin prior to its action, another important but unexplored factor influencing our IR studies. It has been widely believed that the soluble irisin is released from the membrane associated FNDC5 by proteolytic cleavage of its C-terminal moiety and then entered into the extracellular space (2012, Nature 481, 463–468). ***The results from ours and others however, lead us to question this model and investigate the extent to which irisin is existed and circulated as the intact FNDC5.*** FNDC5 has a signal peptide, a single fibronectin type III domain, and a hydrophobic domain that is likely to be membrane anchored. Aside from proteolytic cleavage to release the soluble protein, extracellular vesicle (EV) is another increasingly appreciated way to secret proteins into the extracellular space through the release of the membrane vesicle (2013, J. Cell Biol. 200, 373–383). Therefore, we briefly explored the possibility of the release of intact FNDC5 as EV instead soluble irisin into the plasma. In preliminary studies, we transfected HEK293 cells with a vector expressing the full length FNDC5 gene, and then isolated the EV after ultracentrifuging cell culture medium (100,000 g for 1 hour). The isolated EV samples were then analyzed in western blotting to detect FNDC5 or irisin using irisin antibody. The study found clear bands at approximately 34 kDa whose intensity increased from day 1 to 3 (**Fig. 10A**). From the EV collected from the culture medium of HEK293 cells transfected with the empty vector, this band was absent. Interestingly, the size of this band at 34 kDa is consistent with the previously reported size of irisin detected from the mice plasma. This result therefore suggested that FNDC5 can be secreted as the EV. To further examine this result, a *GFP* reporter gene was fused to the C-terminus of *FNDC5* and the resultant construct was used to transfect HEK293 cells. Using confocal high resolution microscopy, we did observe the accumulation of green fluorescence in small vesicles (**Fig. 10B**). Overall, ***our preliminary data implied the existence of FNDC5 in the EV.*** Compared with soluble proteins, the EVs have highly different ways to interact with target cells and cellular targets of proteins in the EVs can be intracellular, instead on the cell membrane, in principle agreeing with the discovery of the recent paper (*Sci Transl Med*. 2017 Nov 29; 9(418). pii: eaao6298.). Therefore, irisin in the body may exist as intact FNDC5 in the EVs that are then circulated to different organs or interact with nearby organs. Such a scenario can well explain the low binding ability of r-irisin to 3T3-L1 adipocytes, the little-to-no harvest of IR crosslinking products (**Figs. 2D**, **8B**, and **9**), and the varying but generally low levels of irisin in biological samples. Importantly, the secretion of intact FNDC5 in the EVs likely indicates that the receptor of irisin is ***intracellularly located***, paving the solid foundation toward the isolation and identification of this critical but elusive component of irisin signaling. ***Additional support to this new research direction will be of significance and impact to the development of irisin-based approaches for the treatment and management of obesity and diabetes.***

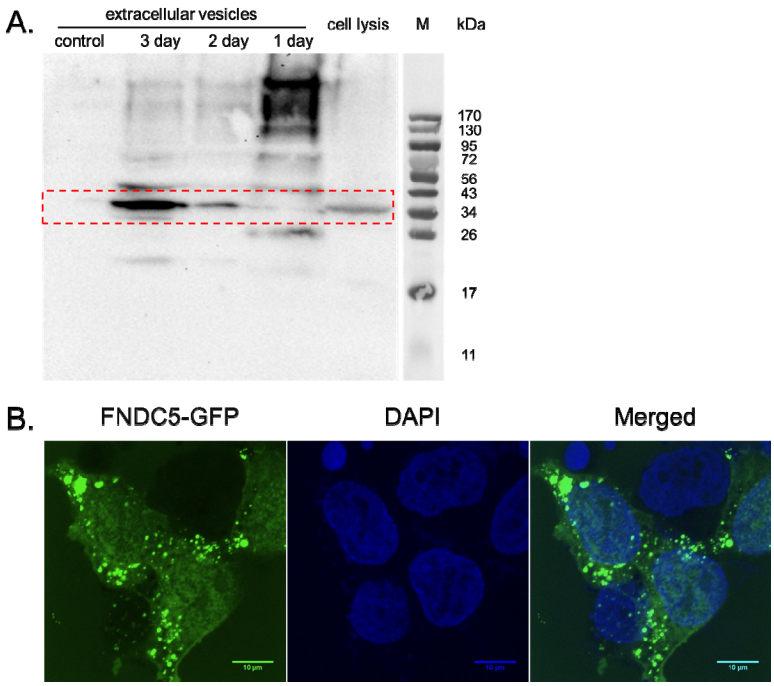

Fig. 10. A: Western blotting analysis of FNDC5 in extracellular vesicles of HEK293/FNDC5 and HEK293 (control), and cell lysis of HEK293/FNDC5. **B:** Fluorescence microscopy of HEK293/FNDC5-GFP.

5.2. Actual or anticipated problems or delays and actions or plans to resolve them.

As described in the section 5.1, we did not observe the cross-linked products after incubating UAA-labeled e-irisin variants with differentiated 3T3-L1 cells. Such an unanticipated problem delayed our progress in the isolation and identification of IR. Fortunately, our preliminary results suggested that the IR might not be located on cell surface. Instead, irisin may exist as the intact FNDC5 in the EV that might be internalized into the receiving cells to initiate the signaling pathway of irisin, leading to adipocyte browning.

5.3. Changes that had a significant impact on expenditures.

Nothing to Report.

5.4. Significant changes in use or care of human subjects, vertebrate animals, biohazards, and/or select agents.

Nothing to Report.

5.5. Significant changes in use or care of human subjects.

Nothing to Report.

5.6. Significant changes in use or care of vertebrate animals.

Nothing to Report.

5.7. Significant changes in use of biohazards and/or select agents.
Nothing to Report.

6. Products

6.1. Publications, conference papers, and presentations.

Publication:

Zhang Y, Xie C, Wang H, Foss R, Clare M, George EV, Li S, Katz A, Cheng H, **Ding Y**, Tang D, Reeves WH, **Yang LJ**. Irisin exerts dual effects on browning and adipogenesis of human white adipocytes. *Am J Physiol Endocrinol Metab*. 2016, 311(2):E530-41.

Presentations:

1. Yousong Ding. Interdisciplinary Approaches in Drug Research. Chemistry Club, University of Florida. Jan 27th, 2017.
2. Li-jun Yang. Veterinary medical school at Louisiana State University. September 15th, 2016.
3. Yousong Ding. Beneficial Effects of Irisin on Human Health. Annual Meeting of American Chemical Society Florida Section, Tampa, FL May 5th to 7th, 2016.
4. Yousong Ding. Drugs, Engineering, and Evolution for Better. Chemistry Club, University of Florida. February 4th, 2016.
5. Yousong Ding. Chemistry, Engineering, and Evolution for Better. Science for Life, University of Florida. November 11th, 2015.

6.2. Website(s) or other Internet site(s)

Nothing to report.

6.3. Technologies or techniques

Nothing to report.

6.4. Inventions, patent applications, and/or licenses

Nothing to report.

6.5. Other Products

Nothing to report.

7. Participants & Other Collaborating Organizations

7.1. What individuals have worked on the project?

The project ran from July 1st, 2015 to Dec 31st, 2016, and then received a no-cost extension from Jan 1st, 2017 to Dec 31st, 2017. The following individuals received the support from this program during the initial 18-month award period but not the next 12 months.

Name:	Yousong Ding
Project Role:	PI
Researcher Identifier:	
Nearest person month worked:	2.7

Contribution to Project:	Dr. Ding is responsible for the overall administration and direction of the project. He is directing the chemical biology and –omics aspects of the project, and supervising one postdoctoral research fellow to create and characterize irisin variants, perform -omics studies, identify irisin receptor, analyze the results, and disseminate data.
Funding Support:	

Name:	Li-jun Yang
Project Role:	Collaborating Investigator
Researcher Identifier:	
Nearest person month worked:	0.72
Contribution to Project:	Prof. Yang is directing the in vitro activity tests of engineered irisin variants created in the Ding Lab
Funding Support:	

Name:	Guang Yang
Project Role:	Postdoctoral Scholar
Researcher Identifier:	
Nearest person month worked:	11.8
Contribution to Project:	Dr. Yang is responsible for irisin production, UAA incorporation into irisin and verification, expression optimization, and proteomic analysis development and optimization.
Funding Support:	

Name:	Shiwu Li
Project Role:	Senior Research Scientist
Researcher Identifier:	
Nearest person month worked:	3.6
Contribution to Project:	Dr. Li is responsible for cell culturing and differentiation, EV studies, in vitro cell-based activity testing of engineered irisin analogs.
Funding Support:	

7.2. Has there been a change in the active other support of the PD/PI(s) or senior/key personnel since the last reporting period?

Nothing to report.

7.3. What other organizations were involved as partners?

Nothing to report.

8. Specific Reporting Requirements

Not applicable.

9. Appendices

A publication in *Am J Physiol Endocrinol Metab*. 2016, 311(2):E530-41.

Am J Physiol Endocrinol Metab 311: E530–E541, 2016.
First published July 19, 2016; doi:10.1152/ajpendo.00094.2016.

Irisin exerts dual effects on browning and adipogenesis of human white adipocytes

Yuan Zhang,[1,2] Chao Xie,[1] Hai Wang,[1] Robin M. Foss,[1] Morgan Clare,[1] Eva Vertes George,[1] Shiwu Li,[1] Adam Katz,[3] Henrique Cheng,[4] Yousong Ding,[5] Dongqi Tang,[2] Westley H. Reeves,[6] and Li-Jun Yang[1]

[1]*Department of Pathology, Immunology, and Laboratory Medicine, University of Florida College of Medicine, Gainesville, Florida;* [2]*Center for Stem Cell and Regenerative Medicine, The Second Hospital of Shandong University, Jinan, China;* [3]*Department of Surgery, University of Florida College of Medicine, Gainesville, Florida;* [4]*Department of Comparative Biomedical Sciences, School of Veterinary Medicine, Louisiana State University, Baton Rouge, Louisiana;* [5]*Department of Medicinal Chemistry, Center for Natural Products, Drug Discovery, and Development, College of Pharmacy, University of Florida, Gainesville, Florida; and* [6]*Department of Medicine, University of Florida College of Medicine, Gainesville, Florida*

Submitted 17 March 2016; accepted in final form 8 July 2016

Zhang Y, Xie C, Wang H, Foss RM, Clare M, George EV, Li S, Katz A, Cheng H, Ding Y, Tang D, Reeves WH, Yang LJ. Irisin exerts dual effects on browning and adipogenesis of human white adipocytes. *Am J Physiol Endocrinol Metab* 311: E530–E541, 2016. First published July 19, 2016; doi:10.1152/ajpendo.00094.2016.—To better understand the role of irisin in humans, we examined the effects of irisin in human primary adipocytes and fresh human subcutaneous white adipose tissue (scWAT). Human primary adipocytes derived from 28 female donors' fresh scWAT were used to examine the effects of irisin on browning and mitochondrial respiration, and preadipocytes were used to examine the effects of irisin on adipogenesis and osteogenesis. Cultured fragments of scWAT and perirenal brown fat were used for investigating signal transduction pathways that mediate irisin's browning effect by Western blotting to detect phosphorylated forms of p38, ERK, and STAT3 as well as uncoupling protein 1 (UCP1). Individual responses to irisin in scWAT were correlated with basal expression levels of brown/beige genes. Irisin upregulated the expression of browning-associated genes and UCP1 protein in both cultured primary mature adipocytes and fresh adipose tissues. It also significantly increased thermogenesis at 5 nmol/l by elevating cellular energy metabolism (OCR and ECAR). Treating human scWAT with irisin increased UCP1 expression by activating the ERK and p38 MAPK signaling. Blocking either pathway with specific inhibitors abolished irisin-induced UCP1 upregulation. However, our results showed that UCP1 in human perirenal adipose tissue was insensitive to irisin. Basal levels of brown/beige and *FNDC5* genes correlated positively with the browning response of scWAT to irisin. In addition, irisin significantly inhibited adipogenic differentiation but promoted osteogenic differentiation. We conclude that irisin promotes "browning" of mature white adipocytes by increasing cellular thermogenesis, whereas it inhibits adipogenesis and promotes osteogenesis during lineage-specific differentiation. Our findings provide a rationale for further exploring the therapeutic use of irisin in obesity and exercise-associated bone formation.

irisin; adipocytes browning; adipogenesis; osteogenesis; human white adipose tissue; brown adipose tissue; thermogenesis

METABOLIC COMPLICATIONS OF OBESITY, including metabolic syndrome and type 2 diabetes mellitus, are worldwide health problems. Obesity results from excessive energy intake compared with energy expenditure, leading to increased adipose tissue mass and ectopic fat accumulation. Brown adipose tissue (BAT), a thermogenic tissue, consumes energy as heat, which is otherwise stored by white adipose tissue (WAT) (30). The thermogenic capability of BAT is mediated by mitochondria uncoupling protein 1 (UCP1), which uncouples the electron transport chain from energy production, resulting in heat production (39). Remarkably, the mass of BAT shows an inverse correlation with body mass index (BMI) and adiposity (9, 13). Thus, by increasing the amount and/or activity of BAT, energy consumption can be increased, and this may serve as a potential therapeutic strategy for obesity and its associated complications.

Irisin, an exercise-induced myokine in mice and humans, promotes "browning" of subcutaneous (sc) white adipocytes by increasing the expression of mitochondrial UCP1 (5). The precursor of irisin is full-length fibronectin type III domain containing 5 (FNDC5), whose overexpression protects high-fat diet-induced obesity in mice by promoting formation of beige (brite) adipocytes (5). Recently, we found that in obese mice, recombinant irisin (r-irisin) stimulates browning of white adipocytes via extracellular signal-related kinase (ERK) and p38 mitogen-activated protein kinase (MAPK) signaling, causing weight loss and improved insulin sensitivity (49). Thus, irisin may be an attractive target for fighting obesity and diabetes (16, 45).

Although beneficial effects of irisin have been observed in animals, the existence of circulating irisin in humans is controversial due to doubts surrounding the ATA translation start codon in human FDNC5 (35), the reliability of irisin antibodies (18), and experimental evidence that commercial irisin ELISA kits are unreliable (2). However, a recent study has put this controversy to rest by confirming the presence of irisin in human plasma and its elevation after exercise using quantitative mass spectrometry (24). Nevertheless, the browning effect of irisin in human adipocytes remains controversial (23, 26, 35). In addition, the ability of exercise per se to stimulate fat browning in humans is still being debated (14, 43). In this study, we systematically examined the effects of irisin on browning of human primary mature white adipocytes and fresh human scWAT as well as on adipose tissue-derived preadipocytes (stem-like cells) during lineage-specific differentiation. Compared with primary white adipocytes, scWAT fragments represent largely native fat tissue. Our data suggest that irisin increases the expression of beige genes and the UCP1 protein (known as "browning") in both human primary mature white adipocytes and fresh human scWAT. This browning

Address for reprint requests and other correspondence: L. J. Yang, Dept. of Pathology, Immunology, and Laboratory Medicine, Univ. of Florida College of Medicine, Gainesville, FL 32610 (e-mail: yanglj@pathology.ufl.edu).

effect is mediated through the p38/ERK MAPK signaling pathways. Treatment of mature white adipocytes with irisin significantly increased cellular thermogenesis. Our data suggest a positive correlation between basal levels of beige gene expression in scWAT and the levels of UCP1 expression of these tissues in response to irisin. Additionally, irisin inhibited adipogenesis during differentiation, supporting its dual roles in converting the mature energy-storing white adipocytes into energy-burning beige adipocytes and suppressing new adipocyte formation. Furthermore, irisin also promoted osteogenic differentiation. To our knowledge, this is the first systematic study of the mechanisms of irisin's effects in human adipose tissue and adipocytes. The data lay the groundwork for further investigating the therapeutic usage of irisin.

METHODS

Production of r-irisin. Production of r-irisin in yeast was performed as described previously (46, 49).

Harvest of scWAT and perirenal BAT. Human scWAT from breast fat of 28 female donors ages 17–73 yr and perirenal BAT from four donors (3 males and 1 female) were obtained from surgical specimens through the University of Florida, Department of Pathology Grossing Room, according to a protocol approved by the Institutional Review Board. All scWAT donors were females undergoing breast reduction for cosmetic reasons, and all perirenal fat donors were undergoing nephrectomy due to malignancy (renal cell carcinoma). Fat tissues were processed within 6 h after surgery. Adipose tissue (2–5 g/donor) was dissected from surrounding fibrous-vascular tissue and cut into 2- to 3-mm pieces. Adipose tissue fragments were used to obtain preadipocytes from mature adipocytes by ceiling culture or placed directly in flasks for tissue culture. Since a variable amount of adipose tissue was obtained from donors, we triaged our experiments based on sample availability, aiming at five to six donors per group.

Isolation and expansion of human primary preadipocytes. Isolation and expansion of preadipocytes from human scWAT were performed as described with minor modifications (Fig. 1) (19). Briefly, fresh fat tissue fragments were cultured in T25 flasks filled with basic medium (BM; DMEM-F-12 medium + 10% fetal bovine serum, 100 U/ml penicillin-streptomycin). Fat tissue floated to the top surface of the flask ("ceiling" cultures), and mature adipocytes were attached to the top of the flasks. Preadipocytes dedifferentiated from mature adipocytes were split at ~70% confluence at a 1:4 ratio for three to four passages to generate sufficient cells for our experiments, which usually took 2–4 mo.

Differentiation of human preadipocytes into mature adipocytes and osteoblasts. Preadipocytes derived from mature adipocytes are known to possess mesenchymal stem cell (MSC) properties and exhibit multilineage differentiation capacity (20). Human preadipocytes were cultured in six-well plates until confluent and then induced toward adipogenic differentiation in differentiation medium (DM; BM + 0.5 mmol/l isobutylmethylxanthine, 0.25 μmol/l dexamethasone, and 10 μmol/l insulin) for 14 days, with fresh medium added every 3rd day. After 14 days, cells were treated with irisin or vehicle for 4 more days to examine whether irisin can induce browning in human mature adipocytes. For osteogenic differentiation, the DM was composed of BM + 0.1 μmol/l dexamethasone, 0.2 mmol/l ascorbic acid, and 10 mmol/l β-glycerophosphate. Irisin was included in the DM for the entire differentiation period to demonstrate the effect of irisin in osteogenesis. Adipogenic and osteogenic differentiation was confirmed by Oil Red O and alizarin red staining (34).

Mitochondrial bioenergetics analysis. Preadipocytes were differentiated into mature adipocytes in adipogenic DM for 14 days and then seeded into XF96 Microplates (15,000/well) for 3–4 days in the absence/presence of various irisin concentrations, rosiglitazone (Sigma-Aldrich), or CL316243 (Sigma-Aldrich). Metabolic analyses were performed using a Seahorse Bioscience XF96 Analyzer, which enables real-time simultaneous measurement of oxygen consumption rate (OCR) and extracellular acidification rates (ECAR). Following basal respiration, the mitochondrial effectors (oligomycin, FCCP, and rotenone) were injected sequentially according to our previously established protocols (46).

Western blotting. Anti-phosphroylated (p)-ERK1/2 (no. 9101), anti-p-p38 MAPK (no. 9211), and anti-p-STAT3 (no. 9145) antibodies (Cell Signaling Technology), anti-β-actin (A5316; Sigma-Aldrich), and rabbit anti-UCP1 (AB155117; Abcam) were used for Western blotting. Immunoreactive bands were quantified by densitometry (6, 13).

RNA isolation and quantitative real-time PCR. Quantitative RT-PCR was performed with β-actin RNA as an internal control by the $2^{-\Delta\Delta C_T}$ method (46, 49). Primer sequences are available upon request.

Immunocytochemistry and immunofluorescence. Adipocytes were fixed with 4% parformaldehyde for 10 min and blocked in the presence of hydrogen peroxide. Cells were incubated with anti-UCP1 antibody (1:500) overnight at 4°C. After washing, the cells were incubated with horseradish peroxidase-conjugated [for immunocytochemistry (ICC)] or Alexa fluor 555-conjugated [for immunofluorescence (IF)] secondary antibody (1-h, 22°C). Nuclei were stained by hematoxylin (ICC) or 4,6-diamidino-2-phenylindole (DAPI; IF).

Adipose tissue culture and browning factors treatment. Fresh human scWAT fragments were cultured overnight in 12-well plates in BM to restore quiescence. For short-term signaling, scWAT fragments were bathed in BM containing either irisin (50 nmol/l), vehicle, or rosiglitazone (1 μmol/l) or CL316243 (1 μmol/l) for various times with agitation. For browning, scWAT fragments were bathed in BM containing irisin (0.5, 5, or 50 nmol/l) for various times (2, 3, or 4 days) with agitation. Total proteins and RNAs were collected for Western blotting of UCP1 and qRT-PCR gene expression studies.

Statistical analysis. Results are presented as means ± SE of at least three independent experiments. Each experiment was conducted in triplicate. Statistical significance among multiple groups was analyzed using Prism 5 software by one-way ANOVA, followed by post hoc analyses, and between two groups by Student's *t-test.* $P < 0.05$ was considered significant.

RESULTS

Irisin has browning effects on human mature adipocytes derived from scWAT. Human white adipocytes obtained by "ceiling" culture after 3-day culture exhibited mature adipocyte features, including cytoplasmic lipid droplets and dedifferentiated into spindle-shaped MSC-like preadipocytes. The preadipocytes were expanded and redifferentiated into mature adipocytes following 14-day culture in adipogenic DM. Most cells differentiated into mature adipocytes, as evidenced by cytoplasmic lipid droplets (phase) and Oil Red O-stained lipid droplets (Fig. 1, *A–C*).

We next examined irisin's browning effect on mature primary adipocytes differentiated from preadipocytes of six donors' scWAT (*donors 1–6*; Fig. 1*D*). After adipogenic differentiation, adipocytes treated with irisin (50 nmol/l) for 4 days showed upregulation of browning-related genes (*UCP1*, *PGC1A*, and *PRDM16*) but exhibited individual differences. In contrast, the expression of general adipose genes (*PPARG* and *ADIPOQ*) showed no difference between the control and irisin groups (not shown). Next, we analyzed UCP1 protein expression after irisin treatment by ICC (Fig. 1*E*) and IF (Fig. 1*F*). UCP1 expression was enhanced and the percentage of UCP1-positive cells increased (57 vs. 12% in control group), strongly suggesting that irisin induced browning of mature adipocytes, consistent with the observations of Lee et al. (26).

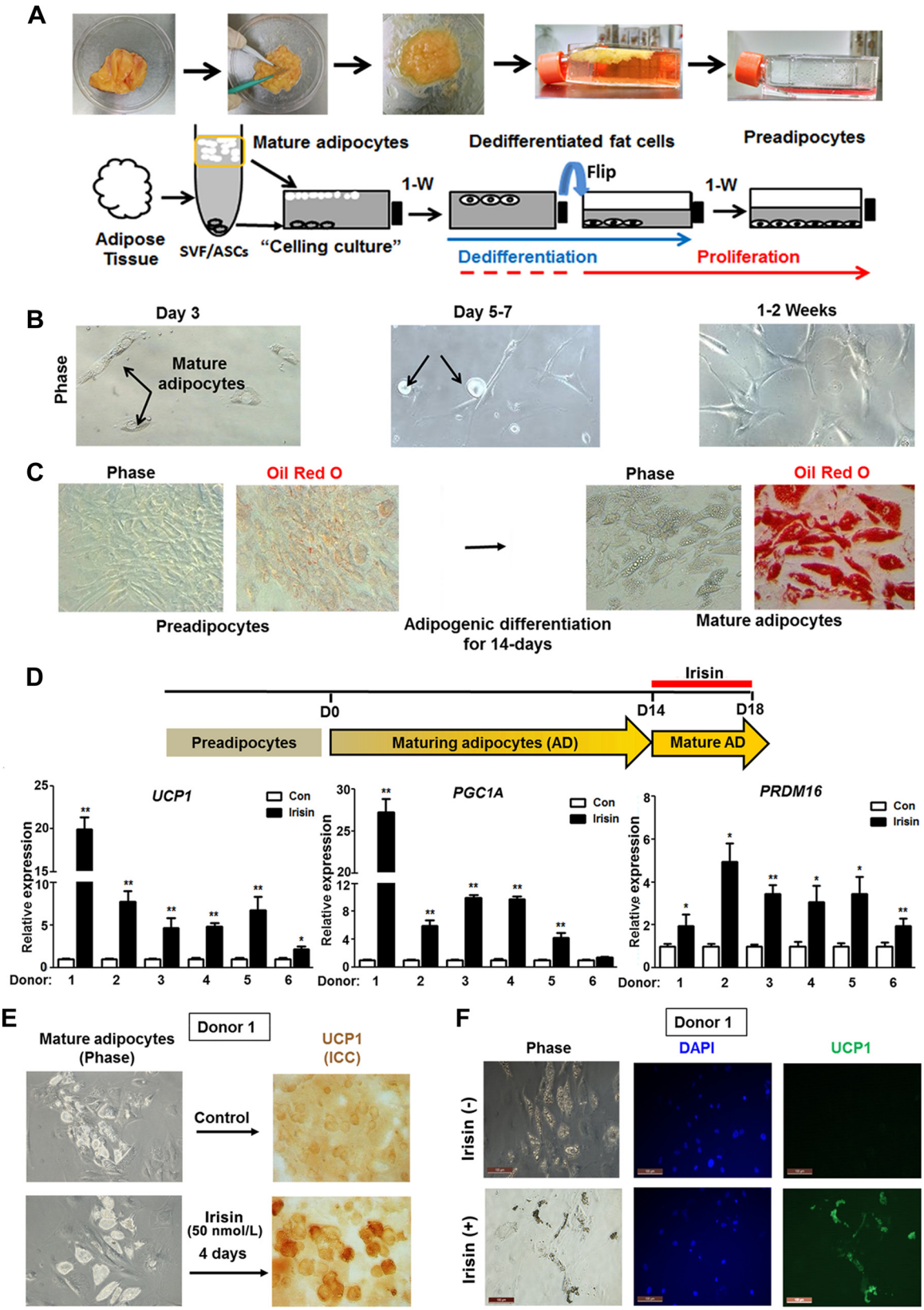

Fig. 1. Irisin has browning effects on mature adipocytes. *A*: derivation of human preadipocytes. Preadipocytes were derived from human subcutaneous white adipose tissue (scWAT) by dissection and "ceiling" culture and then flipped over for expansion. *B*: morphological changes of adipocytes dedifferentiated into preadipocytes. *C*: phase and Oil Red O staining of preadipocytes and mature adipocytes after 14 days of adipogenic differentiation. *D*: irisin treatment upregulated expression of browning-related genes *UCP1* (uncoupling protein 1), *PGC1A* (peroxisome proliferator-activated receptor-γ coactivator-1α), and *PRDM16* (PR domain-containing 16) (*$P < 0.05$, **$P < 0.01$ vs. control). *E* and *F*: irisin enhanced browning of mature adipocytes; UCP1 protein detected by immunocytochemistry (ICC) and immunofluorescence (IF). SVF/ASCs, stromal vascular fraction/adipose-derived stromal/stem cells; DAPI, 4,6-diamidino-2-phenylindole.

Irisin increased thermogenesis of human mature adipocytes. To examine effects of irisin on thermogenesis in mature adipocytes isolated from scWAT, we measured mitochondrial respiration. Figure 2 shows that irisin increased OCR (Fig. 2, *A* and *B*) and ECAR (Fig. 2, *C* and *D*) at effective concentrations as low as 5 nmol/l. Mitochondrial respiration (OCR) of irisin-treated adipocytes was different from that of untreated controls or low dose of irisin-treated cells. In contrast to 0.5 nmol/l irisin, adipocytes treated with 50 nmol/l irisin showed increased basal, uncoupled (oligomycin), and maximal (FCCP) mitochondrial respiration, whereas 5 nmol/l irisin increased basal and uncoupled cellular respiration but not maximal mitochondrial respiration. Adipocytes treated with irisin (5 or 50 nmol/l) also increased glycolysis (ECAR). These data demonstrated that irisin increased cellular thermogenesis by upregulating UCP1, uncoupling oxidative phosphorylation from ATP synthesis, resulting in energy dissipation in the form of heat (15).

Irisin upregulated UCP1 expression in scWAT by activating ERK/p38 MAPK signaling. The potentially beneficial effects of irisin-mediated browning on human adipocytes led us to probe its potential therapeutic significance. Although assessing irisin's effects directly in human subjects was impractical, fresh human scWAT fragments are suitable for modeling irisin's functions. Our previous murine studies show that irisin activates p38 MAPK and ERK signaling (49). As shown in Fig. 3, *A* and *B*, phosphorylation of p38 MAPK (p-p38) and ERK (p-ERK) was enhanced by irisin treatment for 60 min. In five donors (*donors 7–11*), irisin increased p-ERK 2.37 ± 0.41-fold at 60 min and 2.74 ± 0.25-fold at 90 min. p-p38 Levels increased similarly, whereas p-STAT3 was unchanged. To verify the involvement of p38/ERK signaling in UCP1 expression, scWAT fragments were treated with p-p38 (SB-203580) or p-ERK (U-0126) inhibitor for 30 min, followed by irisin. Both abolished irisin-induced upregulation of UCP1 protein (Fig. 3*C*), suggesting that activation of p38/ERK MAPK signaling is required for UCP1 expression.

In human adults, adipocytes derived from perirenal adipose tissue were smaller and expressed higher UCP1 compared with scWAT, suggesting that perirenal fat in human adults acts as brown adipose tissue (27, 29, 41). We also examined whether irisin regulates human perirenal fat, which is classified as BAT. Figure 3*D* shows that the ERK and p38 were already phosphorylated in untreated perirenal fat and that irisin did not enhance further phosphorylation. Further irisin treatment did not affect UCP1 translation ($n = 4$; Fig. 3, *E* and *F*) or *UCP1* and *PRDM16* transcription ($n = 3$; Fig. 3*G*). Thus, our study suggests that human BAT from perirenal fat has high levels of UCP1 protein, and its regulation appears to be irisin independent.

Next, we explored irisin's browning effect in scWAT fragments. Treatment of scWAT with irisin for 4 days increased UCP1 protein (Fig. 4*A*) and brown-associated transcripts (*UCP1 and PRDM16*; Fig. 4*B*) in >75% of scWAT samples. Interestingly, two irisin nonresponders (*donors 13* and *17*) had relative higher levels of basal UCP1 protein than the irisin responders, suggesting that these fat tissues might be blended

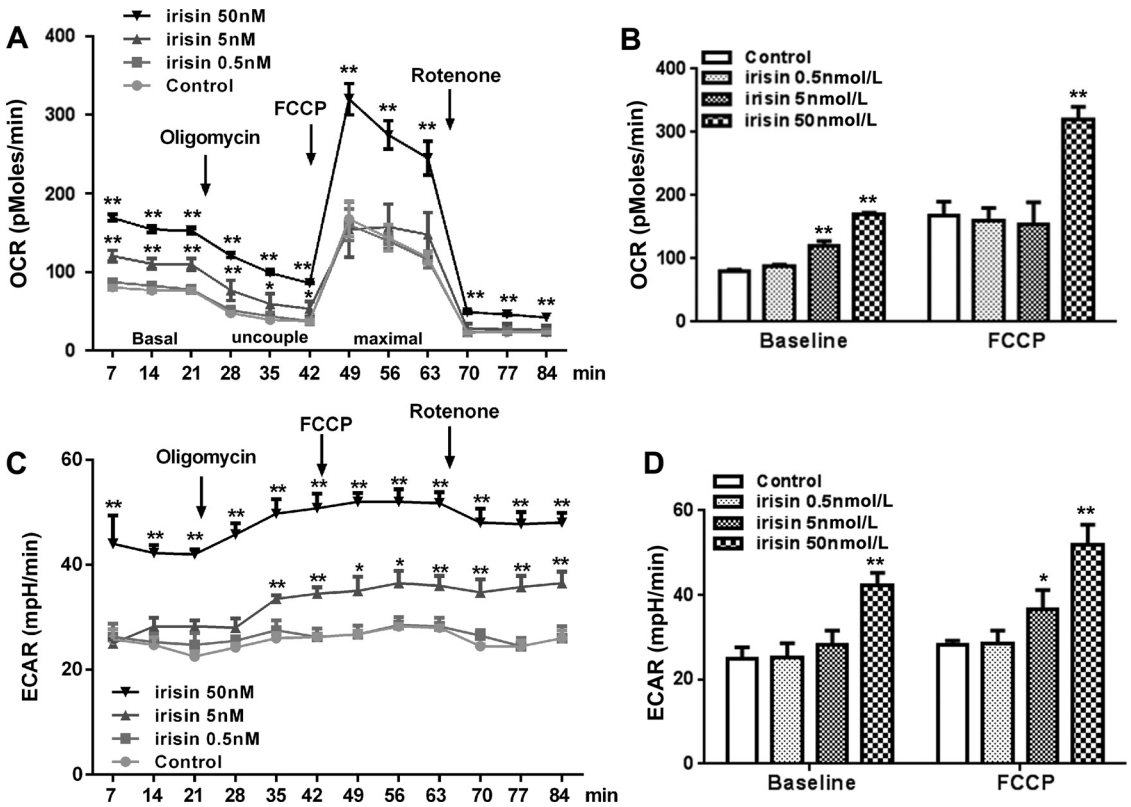

Fig. 2. Effects of irisin on adipocyte thermogenesis. scWAT mature adipocytes were incubated with/without irisin for 4 days. Oligomycin and FCCP were used for determining uncoupled and maximal mitochondrial respiration, respectively. Effects of irisin on cellular oxygen consumption rate (OCR; *A* and *B*) and ECAR (extracellular acidification rates; *C* and *D*) were measured by XF96 Analyzer. Experimental treatments were performed with 6 technical replicates and 4 biological replicates. **P* ± 0.05 and ***P* ± 0.01 vs. control.

AJP-Endocrinol Metab • doi:10.1152/ajpendo.00094.2016 • www.ajpendo.org

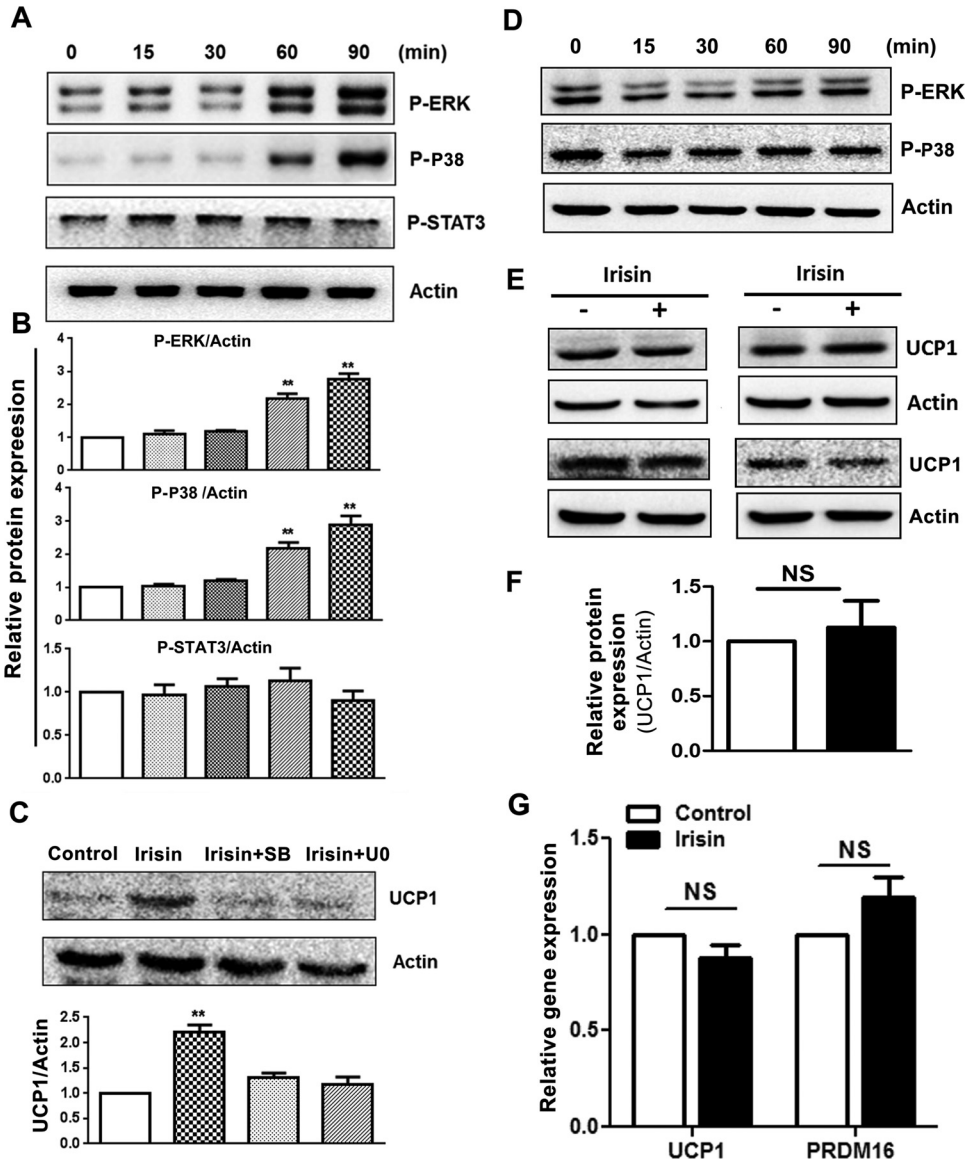

Fig. 3. Irisin activates p38/ERK MAPK signaling pathways in scWAT. *A* and *B*: fresh scWAT fragments from *donors 7–11* were treated with irisin (50 nmol/l) for the indicated time, and protein extracts were probed by Western blotting. Levels of phosphorylated (p)-ERK, p-p38, and p-STAT3 were quantified by densitometry, corrected with β-actin, and normalized against the untreated control. *C*: increased UCP1 is mediated by p38/ERK. Inhibitors of p-p38 [SB-203580 (SB)] or p-ERK [U0126 (U0)] were added 30 min before irisin was added to scWATs of *donors 9–11*. *Donor 10* UCP1 blot is shown. Quantification of UCP1 was similar to that in *B*. *D–G*: fresh perirenal BAT fragments from *donors 29* to *32* (3 males and 1 female) were treated with irisin (50 nmol/l) at different time points for detection of p-p38 and p-ERK (*D*) or at 4 days (*E–G*) for UCP1 expression. *F*: densitometry quantification of UCP1. *G*: *UCP1* and *PRDM16* transcripts. Data are expressed as means ± SE of 3 donors. NS, no significance, irisin-treated vs. control.

with BAT. Interestingly, irisin treatment of scWAT increased *FNDC5* transcript in all donors except for *donor 13*, suggesting positive autoregulation of irisin, in agreement with previous studies (11, 37).

To determine the lowest effective dose and shortest duration of irisin treatment, we examined the dose response and time course. As shown in Fig. 4*C*, irisin increased UCP1 protein (1- and 3-fold at 5 and 50 nmol/l, respectively, $P < 0.01$). Surprisingly, as early as *day 2* of irisin treatment, UCP1 was increased ($P < 0.01$; Fig. 4*D*), suggesting that irisin plays an early role in UCP1 expression.

Correlation of basal levels of beige gene expression with irisin-induced browning. Responses to irisin can be fat depot specific (5, 26, 45). Given these results and our finding that UCP1 protein levels varied among donors after irisin treatment (Fig. 4*A*), we hypothesized that the genetic background may affect irisin responsiveness. We measured transcription levels of *UCP1* and *PRDM16* in eight donors' scWAT after irisin treatment (Fig. 4*B*). Responsiveness varied considerably, from no response (*donors 13* and *17*) to intermediate (*donors 12* and *15* for *UCP1*, 2- to 4-fold increase) to high responsiveness (*donors 10*, *11*, *14*, and *16*, >10-fold increase). Next, we determined *UCP1*, *TMEM26*, *PRDM16*, *CD137*, and *FNDC5* expression in scWAT from seven donors prior to irisin treatment (scWAT from *donor 10* was insufficient). *CD137* and *TMEM26* are characteristically expressed by beige cells (45). scWAT showed highly variable basal levels of all five genes (Fig. 5*A*), suggesting that the abundance of beige adipocytes in scWAT differs among individuals and that the relative expression changes of *UCP1* and *PRDM16* in irisin-treated scWAT were positively correlated with basal levels of *UCP1*, *TMEM26*, *PRDM16*, *CD137*, and *FNDC5* (Fig. 5*B*). In contrast, the basal levels of *CEBPB* and *ADIPOQ* were similar (not shown). There was no correlation between irisin responsiveness in scWAT and donors' BMI in our limited samples.

Irisin suppressed adipogenic differentiation and promoted osteogenic differentiation. To further explore irisin's contradictory browning effects in human cell models (23, 26, 35), we examined the longitudinal effects irisin treatment during adipogenic or osteogenic differentiation in six donors (*donors 10*

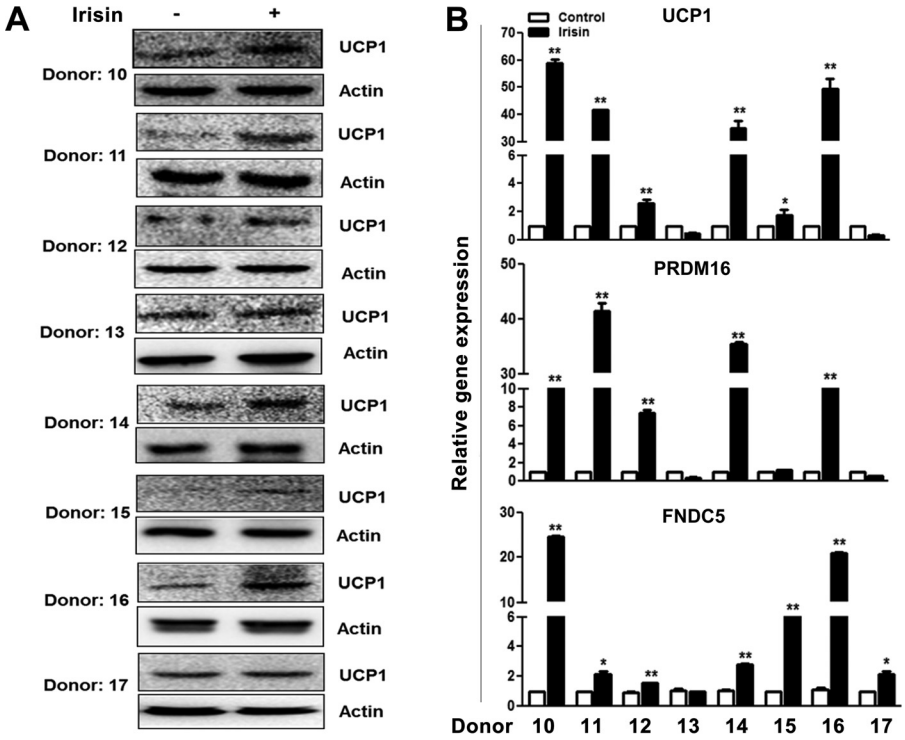

Fig. 4. Irisin upregulates UCP1 expression in scWAT. UCP1 expression in control or 4-day, 50 nmol/l irisin-treated scWAT fragments of 8 donors (*donors 10–17*). *B*: expression of *UCP1*, *PRDM16*, and *FNDC5* genes. *C*: dose response of irisin-stimulated UCP1 expression (*day 4*) in fresh human scWAT. *D*: time course of UCP1 expression. Bar graphs represent UCP1 expression relative to actin (**$P < 0.01$ and *$P < 0.05$ vs. control).

and *18–22*; Fig. 6*A*). After 18 days, mature adipocytes (by morphology and Oil Red O staining) in the irisin-treated group were reduced by 20–60% compared with controls (Fig. 6*B*). Furthermore, irisin decreased *CEBPB* and *ADIPOQ* expression (Fig. 6*C*). *CEBPB* and *ADIPOQ* regulate adipocyte differentiation (25, 44, 48), and suppression of their expression suggests that irisin exerts an inhibitory effect on adipogenesis. This conclusion was further supported by the fact that irisin decreased expression of browning-related *UCP1* and *PRDM16* by 10–65% (Fig. 6*C*). Consistent with the transcription results, UCP1 protein expression was reduced when irisin was included throughout adipogenic differentiation (Fig. 6*D*, *bottom*). In contrast, its level increased dramatically when irisin was included only in the last 4 days (Fig. 6*D*, *middle*). Thus, irisin not only induces browning of mature human adipocytes but also inhibits adipogenic differentiation of preadipocytes. Our data suggest that irisin's browning effect is observed only after formation of mature adipocytes, which may explain, at least partly, the conflicting reports of irisin's effects on human adipocytes.

In addition, we examined irisin's effect on osteogenesis in humans since exercise is known to prevent bone loss and reduce fracture risks. Exposure to irisin (50 nmol/l) during differentiation pushed preadipocytes toward osteoblastic differentiation, as evidenced by mineral deposition highlighted by Alizarin Red staining (Fig. 6*E*), and enhanced the expression of osteogenic genes *RUNX2*, *OSTERIX*, and *OSTEOPONTIN* in five of six donors (Fig. 6*F*). Thus, irisin promotes human osteoblastic differentiation, consistent with recent published murine data (10, 11).

Comparison of "browning" effect among browning factors. PPARG ligand agonists such as rosiglitazone and β_3-adrenergic receptor agonists such as CL316243 can induce a beige fat gene program in scWAT (4). To compare the browning capacity of irisin with traditional browning factors, we tested rosiglitazone and CL-316243. We treated human scWAT fragments from three different donors with 50 nmol/l irisin, 1 μmol/l rosiglitazone, or 1 μmol/l CL316243 for 3 days. As shown in Fig. 7, *A* and *B*, *top*, both UCP1 protein and gene expression were increased significantly after all three treatments, and irisin

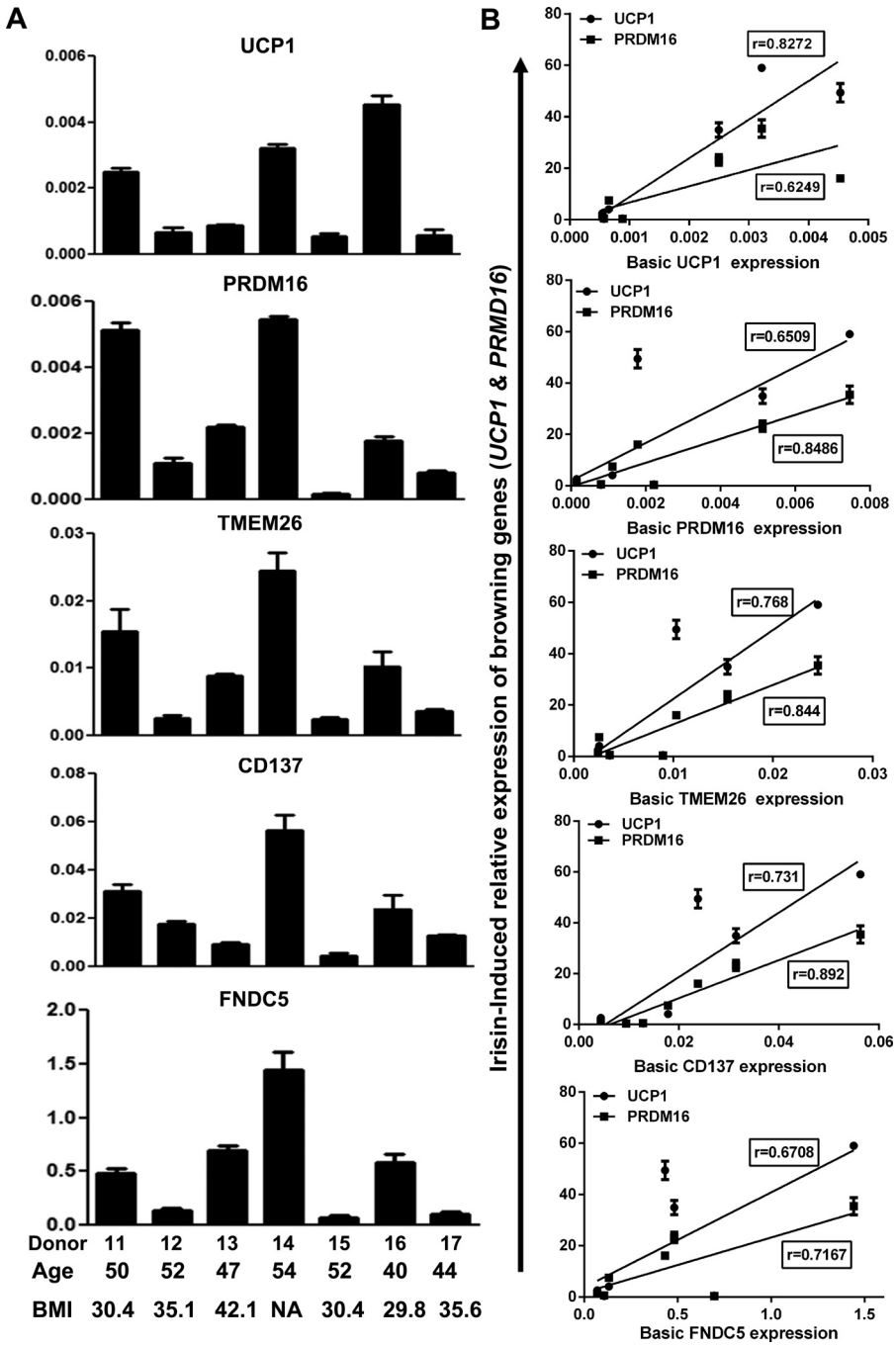

Fig. 5. Correlation of baseline brown gene expression with irisin-mediated browning responsiveness among donors' scWAT. *A*: basal levels of *UCP1*, *PRDM16*, *CD137*, *TMEM26*, and *FNDC5* transcripts in fresh human scWATs of *donors 11–17*. Donors' ages (yr) and BMI (kg/m^2) are listed at the *bottom*. *B*: correlation between basal brown/beige gene expression and levels of irisin-induced *UCP1* and *PRDM16*. ●, Irisin-induced expression of *UCP1*; ■, irisin-induced expression of *PRDM16*, respectively.

seemed more potent on a molar basis than rosiglitazone and CL-316243. In addition, the cotranscriptional regulator PGC1A induces mitochondrial biogenesis by activating nuclear respiratory factors (NRF1 and -2) (32). We found that not only rosiglitazone and CL-316243 but also irisin stimulated *PGC1A* and *NRF1* expression (Fig. 7*B*, *middle* and *bottom*), suggesting that irisin also has a positive effect on mitochondrial biogenesis and cellular metabolism.

Next, we compared the thermogenic effect of rosiglitazone, CL-316243, and irisin on human mature adipocytes isolated from scWAT. Figure 7, *C–E*, shows that both OCR and ECAR at basal and peak levels increased significantly following treatment with irisin, rosiglitazone, or CL-316243. The browning effect of irisin is comparable with rosiglitazone and CL-316243.

DISCUSSION

Animal studies suggest that irisin is an attractive therapeutic target for obesity and metabolic disorders (7, 11, 21, 22, 33, 49). However, its effects in humans are controversial. The present study addressed this gap in our understanding of irisin's action on human fat by using human primary adipocytes and fresh scWAT. We found that *1*) in white adipocytes, irisin upregulated expression of browning-associated genes and UCP1 protein and increased thermogenesis of ma-

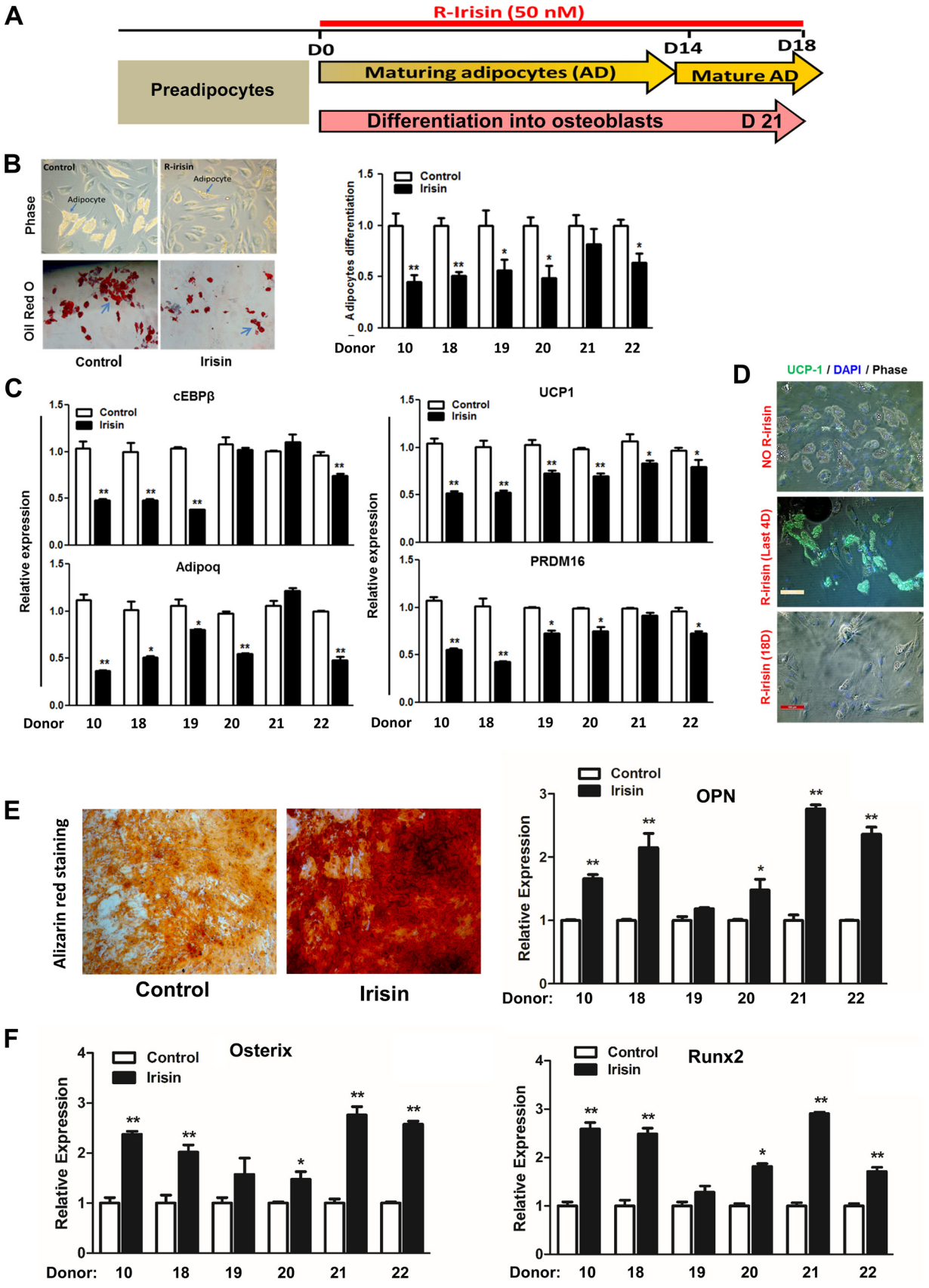

AJP-Endocrinol Metab • doi:10.1152/ajpendo.00094.2016 • www.ajpendo.org

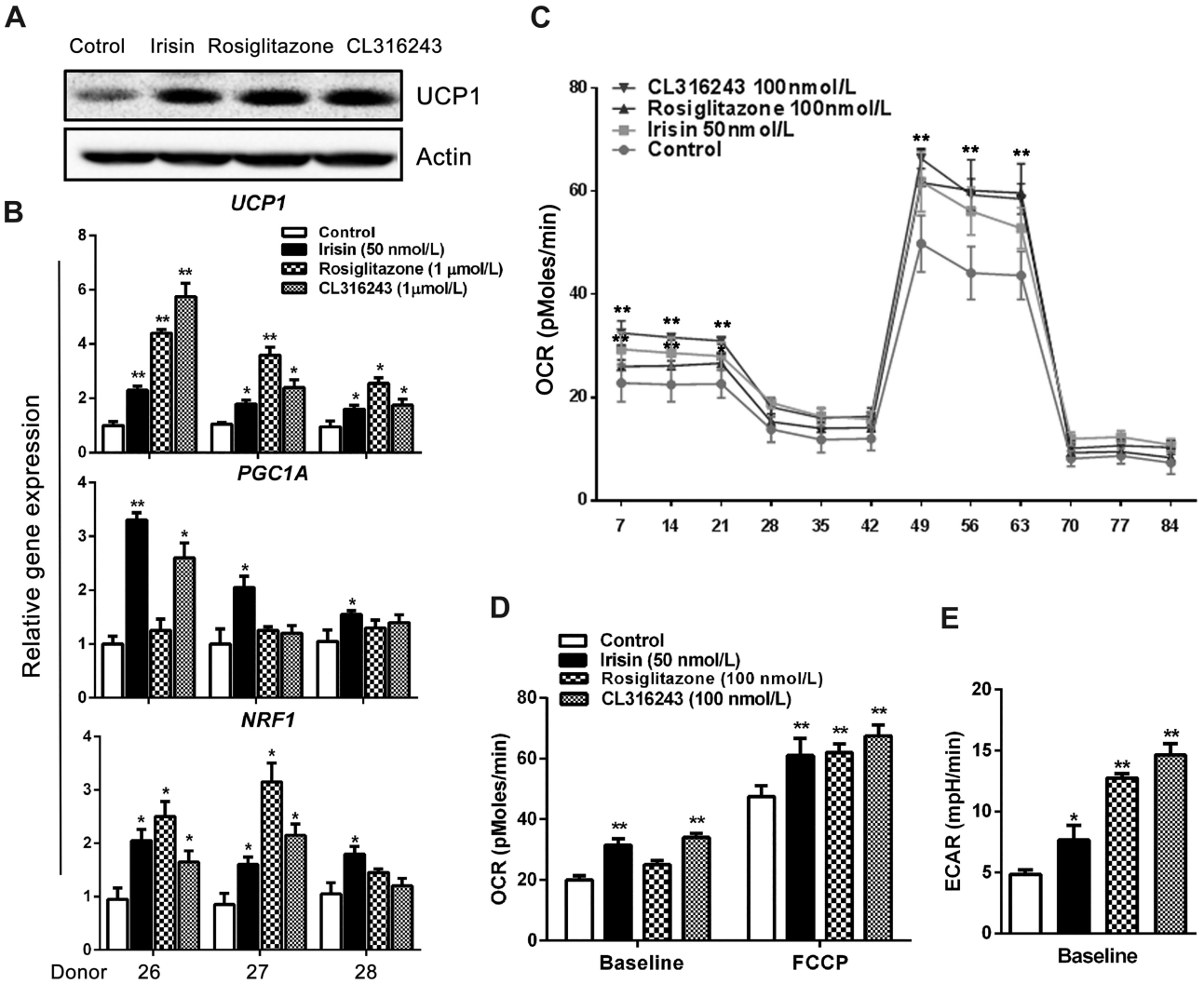

Fig. 7. Comparison of the browning effect by 3 browning reagents. *A* and *B*: human scWAT fragments from breasts of *donors 26–28* were treated with 50 nmol/l irisin, 1 μmol/l rosiglitazone, or 1 μmol/l CL-316243 for 3 days. UCP1 protein level was measured by Western blotting. Bar graphs represent UCP1 expression relative to actin (*A*). *UCP*, *PGC1A*, and *NRF1* mRNA expression was measured by qRT-PCR (*B*). *C–E*: mature human adipocytes were treated with 50 nmol/l irisin, 100 nmol/l rosiglitazone, or 100 nmol/l CL-316243 for 3 days. Then, OCR (*C* and *D*) and ECAR (*E*) were measured by Seahorse XF96 Analyzer. Experimental treatments were performed with 6 technical replicates and 4 biological replicates. $*P < 0.05$ and $**P < 0.01$ vs. control.

ture adipocytes significantly; *2*) this action was mediated by the p38/ERK MAPK pathways since the UCP1 expression was abolished by pathway-specific inhibitors; *3*) the abundance of beige adipocytes in scWATs correlated positively with responsiveness to irisin treatment; *4*) irisin positively autoregulates FDNC5 expression in adipose tissue; and *5*) irisin inhibits adipogenesis, reducing the formation of new adipocytes, and promotes osteoblastic differentiation. These results suggest that irisin may have promising aspects for treatment/prevention of human obesity and osteoporosis.

The browning effects of irisin in humans are controversial. Raschke et al. (35) incubated primary human subcutaneous preadipocytes with FNDC5 and irisin for 18 days and found no browning effect. In contrast, Lee et al. (26) showed that 6-day FNDC5 treatment of human mature adipocytes strongly induced the expression of brown and beige genes. Furthermore, Huh et al. (23) found that browning genes (*UCP1*, *PRDM16*, and *CIDEA)* were induced in human mature adipocytes 8 days after irisin stimulation. These conflicting observations suggest that irisin's browning effects depend on the maturity of adi-

Fig. 6. Irisin inhibits adipogenic and promotes osteogenic differentiation. *A*: preadipocyte differentiation to adipocytes or osteoblasts in the presence of irisin (50 nmol/l) for 18 or 21 days, respectively. *B*: mature adipocytes (arrows) were confirmed by Oil Red O staining (*left*) and mature adipocytes in irisin-treated cells were calculated as %control (*right*). *C*: expression of adipogenic genes (*CEBPB* and *ADIPOQ*) and browning genes (*UCP1* and *PRDM16*) was determined by quantitative RT-PCR (qRT-PCR; $*P < 0.05$ and $**P < 0.01$ vs. control). *D*: cells were stained with anti-UCP1 antibodies and detected by IF. Green, UCP1 protein; blue, DAPI-stained nuclei. Micrographs are merged photos of UCP1, DAPI, and phase images. *E*: differentiated osteoblasts were confirmed by alizarin staining. *F*: the expression of *OPN*, *OSTERIX*, and *RUNX2* genes was determined by qRT-PCR ($*P < 0.05$ and $**P < 0.01$ vs. control). AD, adipocyte.

pocytes. To resolve this, we used two human models, cultured primary mature adipocytes and stem-like preadipocytes, to help reconcile the discrepancy.

Irisin promoted expression of *UCP1* and other brown-related genes in mature adipocytes (Fig. 1), consistent with the findings by Lee et al. (23) and Huh et al. (26). However, opposite effects were obtained when human preadipocytes were induced toward adipogenic differentiation in the presence of irisin during this process (Fig. 6). The marked reduction of mature adipocytes and decreased expression of adipogenic differentiation genes (*CEBPB* and *ADIPOQ*) and BAT-related genes (*UCP1* and *PRDM16*) suggest that irisin exerts inhibitory effects on adipogenesis, and no browning effect was observed if irisin was added during stem cell adipogenic differentiation, which is consistent with the results of Raschke et al. (35). Our studies thus suggest that the effects of irisin in humans are likely differentiation stage dependent. Irisin effectively reprogrammed mature adipocytes into brown-like adipocytes by increasing UCP1 expression (Figs. 1 and 4), and this browning action of irisin is supported further by increased mitochondrial basal, uncoupled, and maximal respiration or thermogenesis following irisin stimulation (Fig. 2). Therefore, our results provide further support for irisin's browning action on mature white adipocytes and scWAT.

Our findings highlight that irisin not only increases cellular thermogenesis by browning scWAT but also reduces fat storage by suppressing formation of new adipocytes. Recently, Xiong et al. (47) demonstrated that irisin increased hormone-sensitive lipase (HSL) expression and reduced perilipin, increasing lipolysis via the cAMP-PKA-HSL/perilipin pathway. This finding may be another possible mechanism by which irisin counters obesity.

The present data contribute to our understanding the role of irisin in human adipose tissue. Adipose tissue consists primarily of mature adipocytes, along with scant stem cells, fibrovascular components, and other cell types, and it has varied roles in regulating metabolism (1). In vitro adipocyte culture is used widely to investigate adipose tissue biology (6), and previous studies of irisin's browning effects have employed this system (23, 26, 35). However, derivation of human primary mature adipocytes involves in vitro dedifferentiation and redifferentiation. The epigenetic changes associated with these processes, the loss of other types of cells, and the lack of three-dimensional structure are limitations of this approach (8, 40). To more accurately evaluate the in vivo therapeutic roles of irisin, we developed a human adipose tissue culture system. As shown in Fig. 4*A*, irisin increased the UCP1 protein in scWAT fragments from different donors to various degrees, and this action was mediated by activating the ERK and p38 MAPK signaling pathways. Inhibition of either pathway with specific inhibitors abolished irisin-stimulated UCP1 protein to baseline levels (Fig. 4*C*), consistent with our murine data (49). Further studies are needed to understand how the activation of these pathways leads to overexpression of UCP1. Nonetheless, our results provide further experimental evidence in support of irisin's browning effect in humans, laying the groundwork for future investigation of the potential therapeutic use of irisin.

Adipose tissues are widespread, and adipocytes at different anatomic locations show different characteristics (3). It is reported that classical brown adipocytes are found in the major dedicated BAT depots of rodents, such as in the interscapular, perirenal, and periaortic regions (38). In human adults, active BAT depots are found in the cervical, supraclavicular, axillary, paravertebral, and perirenal regions (38, 41). Lee et al. (26) showed that FNDC5 (irisin precursor) enhances a BAT-like thermogenic program in neck adipocytes and to a lesser extent subcutaneous adipocytes, but this shows an unclear role in omental visceral adipocytes, suggesting that the response to irisin may be fat depot specific. In our studies, breast scWAT samples showed variable responses of UCP1 expression in response to irisin (Fig. 4), whereas irisin responsiveness, although limited in seven to eight donors, appears to positively correlate with the basal levels of brown and beige adipocyte genes (Fig. 5*A*), suggesting that the abundance of beige adipocytes in scWAT differs among donors, even at the same location. The correlation of irisin-stimulated UCP1 expression with the basal levels of beige-specific genes suggests that beige adipocytes within scWAT are preferentially sensitive to the browning effect of irisin. However, irisin-treated BAT from perirenal fat showed no further activation of p38/ERK MAPK signaling or expression of UCP1/PRDM16 (Fig. 3, *D–G*). The concept of different types of fat cells, in particular different types of thermogenic fat cells, in humans is still very new, and more studies are needed. Our results offer a potential means to assess irisin's therapeutic effects in humans.

In this study, we found that scWAT from breast fat of different donors exhibited individual differences in the extent of irisin-induced UCP1 expression (Fig. 4). To further investigate the reason, the expression of beige genes in different donors was measured. We found that the abundance of beige genes in breast fat differs among individuals. The relative expression changes of UCP1 in irisin-treated breast fat positively correlated with basal levels of *UCP1*, *TMEM26*, *PRDM16*, *CD137*, and *FNDC5* (Fig. 5). In addition, human genetic mutations/variations such as polymorphisms of *UCP1* (−3826A/G) and the *β_3-adrendergic receptor* (*ADRB3*) (64 Trp/Arg) (28, 42) affect beige/brown fat development and energy metabolism, which may be an important reason for the variable responsibility to irisin.

To this end, we compared the browning effect of irisin with that of two well-known agonists, rosiglitazone and CL316243. As shown in Fig. 7, *A* and *B*, treatment of human scWAT fragments with 50 nmol/l irisin, 1 μmol/l rosiglitazone, or 1 μmol/l CL-316243 robustly induced mRNA expression and protein level of UCP1 as well as the mitochondrial biogenesis genes *PGC1A* and *NRF1*. Moreover, treatment of human mature adipocytes with 50 nmol/l irisin, 100 nmol/l rosiglitazone, or 100 nmol/l CL-316243 increased both OCR and ECAR. Although the concentration of rosiglitazone and CL-316243 used was higher than irisin, the browning and thermogenesis effects of irisin were similar to that of the other browning factors. Currently, there is no consensus regarding the physiological range of circulating irisin during rest and exercise (2, 17). Estimates vary from 5 to 1,200 ng/ml in different settings using commercial ELISA kits (12, 31). A recent study examined these ELISA kits and discovered that they lack specificity, casting doubt on the previous measurements of circulating irisin levels (2). In most experiments here, we chose an irisin concentration of 50 nmol/l and at this dose we found a significant browning effect of scWAT at tissue and adipocyte levels. Recently, Jedrychowski et al. (24) confirmed the presence of circulating irisin in human plasma at ~3.6–4.3 ng/ml.

To search for the lowest effective dose of irisin for browning, we examined irisin's effect on mitochondrial respiration and UCP1 expression at 0.5 and 5 nmol/l. We found that at 5 nmol/l, r-irisin from yeast had a browning effect, as evidenced by increased cellular metabolism (Fig. 2) and UCP1 expression (Fig. 4*C*). Although further studies are required to define the exact physiological range of circulating and local irisin, 5 nmol/l used in our study could be considered to be within the physiological range of most circulating hormones and myokines (24), especially considering the low biological activity of recombinant irisin (46). Interestingly, since WAT produces irisin (36), circulating irisin levels may be lower than the local irisin concentration due to paracrine and autocrine regulation.

Because of the limited clinical data available, we could not analyze the correlation of irisin sensitivity with sex, difference percentage of body fat, systolic and diastolic blood pressure, fasting glucose, triglycerides, and HOMA-IR. However, with our limited data, we failed to find any correlation between donors' BMI and the responsiveness to irisin in scWAT.

In conclusion, we found that irisin has significant browning effects on human mature white adipocytes and increases adipocyte thermogenesis. The browning action is mediated via p38/ERK signaling, and irisin responsiveness likely correlates with the numbers of beige adipocytes within scWAT. In contrast, irisin exerts an inhibitory effect on adipocyte formation and promotes osteogenesis during preadipocyte differentiation. Our findings provide experimental evidence supporting the possible therapeutic use of irisin in treating human obesity and osteoporosis.

GRANTS

This work in part supported by research grants from the Lupus Research Institute (L. J. Yang) and Grant 00117544 from Congressionally Directed Medical Research Programs/Department of Defense (Y. Ding and L. J. Yang).

DISCLOSURES

The authors declare no conflict of interest, financial or otherwise.

AUTHOR CONTRIBUTIONS

Y.Z., C.X., H.W., and R.F. performed experiments; Y.Z., M.C., E.V.G., A.K., and L.J.Y. analyzed data; Y.Z. and C.X. prepared figures; Y.Z. drafted manuscript; S.L., H.C., Y.D., D.T., W.H.R., and L.J.Y. edited and revised manuscript; L.J.Y. conception and design of research; L.J.Y. approved final version of manuscript.

REFERENCES

1. **Ahima RS, Flier JS.** Adipose tissue as an endocrine organ. *Trends Endocrinol Metab* 11: 327–332, 2000.
2. **Albrecht E, Norheim F, Thiede B, Holen T, Ohashi T, Schering L, Lee S, Brenmoehl J, Thomas S, Drevon CA, Erickson HP, Maak S.** Irisin - a myth rather than an exercise-inducible myokine. *Sci Rep* 5: 8889, 2015.
3. **Arner P.** Not all fat is alike. *Lancet* 351: 1301–1302, 1998.
4. **Asada R, Kanemoto S, Matsuhisa K, Hino K, Cui M, Cui X, Kaneko M, Imaizumi K.** IRE1alpha-XBP1 is a novel branch in the transcriptional regulation of Ucp1 in brown adipocytes. *Sci Rep* 5: 16580, 2015.
5. **Bostrom P, Wu J, Jedrychowski MP, Korde A, Ye L, Lo JC, Rasbach KA, Bostrom EA, Choi JH, Long JZ, Kajimura S, Zingaretti MC, Vind BF, Tu H, Cinti S, Hojlund K, Gygi SP, Spiegelman BM.** A PGC1-alpha-dependent myokine that drives brown-fat-like development of white fat and thermogenesis. *Nature* 481: 463–468, 2012.
6. **Carswell KA, Lee MJ, Fried SK.** Culture of isolated human adipocytes and isolated adipose tissue. *Meth Mol Biol* 806: 203–214, 2012.
7. **Castillo-Quan JI.** From white to brown fat through the PGC-1alpha-dependent myokine irisin: implications for diabetes and obesity. *Dis Model Mech* 5: 293–295, 2012.
8. **Chen J, Dodson MV, Jiang Z.** Cellular and molecular comparison of redifferentiation of intramuscular- and visceral-adipocyte derived progeny cells. *Int J Biol Sci* 6: 80–88, 2010.
9. **Chondronikola M, Volpi E, Borsheim E, Porter C, Annamalai P, Enerback S, Lidell ME, Saraf MK, Labbe SM, Hurren NM, Yfanti C, Chao T, Andersen CR, Cesani F, Hawkins H, Sidossis LS.** Brown adipose tissue improves whole-body glucose homeostasis and insulin sensitivity in humans. *Diabetes* 63: 4089–4099, 2014.
10. **Colaianni G, Cuscito C, Mongelli T, Oranger A, Mori G, Brunetti G, Colucci S, Cinti S, Grano M.** Irisin enhances osteoblast differentiation in vitro. *Int J Endocrinol* 2014: 902186, 2014.
11. **Colaianni G, Cuscito C, Mongelli T, Pignataro P, Buccoliero C, Liu P, Lu P, Sartini L, Di Comite M, Mori G, Di Benedetto A, Brunetti G, Yuen T, Sun L, Reseland JE, Colucci S, New MI, Zaidi M, Cinti S, Grano M.** The myokine irisin increases cortical bone mass. *Proc Natl Acad Sci USA* 112: 12157–12162, 2015.
12. **Crujeiras AB, Pardo M, Casanueva FF.** Irisin: "fat" or artefact. *Clin Endocrinol* 82: 467–474, 2015.
13. **Cypess AM, Lehman S, Williams G, Tal I, Rodman D, Goldfine AB, Kuo FC, Palmer EL, Tseng YH, Doria A, Kolodny GM, Kahn CR.** Identification and importance of brown adipose tissue in adult humans. *N Engl J Med* 360: 1509–1517, 2009.
14. **Dinas PC, Nikaki A, Jamurtas AZ, Prassopoulos V, Efthymiadou R, Koutedakis Y, Georgoulias P, Flouris AD.** Association between habitual physical activity and brown adipose tissue activity in individuals undergoing PET-CT scan. *Clin Endocrinol* 82: 147–154, 2015.
15. **Divakaruni AS, Brand MD.** The regulation and physiology of mitochondrial proton leak. *Physiology* 26: 192–205, 2011.
16. **Elbelt U, Hofmann T, Stengel A.** Irisin: what promise does it hold? *Curr Opin Clin Nutr Metab Care* 16: 541–547, 2013.
17. **Elsen M, Raschke S, Eckel J.** Browning of white fat: does irisin play a role in humans? *J Endocrinol* 222: R25–R38, 2014.
18. **Erickson HP.** Irisin and FNDC5 in retrospect: An exercise hormone or a transmembrane receptor? *Adipocyte* 2: 289–293, 2013.
19. **Fernyhough ME, Vierck JL, Hausman GJ, Mir PS, Okine EK, Dodson MV.** Primary adipocyte culture: adipocyte purification methods may lead to a new understanding of adipose tissue growth and development. *Cytotechnology* 46: 163–172, 2004.
20. **Fraser JK, Wulur I, Alfonso Z, Hedrick MH.** Fat tissue: an underappreciated source of stem cells for biotechnology. *Trends Biotechnol* 24: 150–154, 2006.
21. **Ghahrizjani FA, Ghaedi K, Salamian A, Tanhaei S, Nejati AS, Salehi H, Nabiuni M, Baharvand H, Nasr-Esfahani MH.** Enhanced expression of FNDC5 in human embryonic stem cell-derived neural cells along with relevant embryonic neural tissues. *Gene* 557: 123–129, 2015.
22. **Hashemi MS, Ghaedi K, Salamian A, Karbalaie K, Emadi-Baygi M, Tanhaei S, Nasr-Esfahani MH, Baharvand H.** Fndc5 knockdown significantly decreased neural differentiation rate of mouse embryonic stem cells. *Neuroscience* 231: 296–304, 2013.
23. **Huh JY, Dincer F, Mesfum E, Mantzoros CS.** Irisin stimulates muscle growth-related genes and regulates adipocyte differentiation and metabolism in humans. *Int J Obes* 38: 1538–1544, 2014.
24. **Jedrychowski MP, Wrann CD, Paulo JA, Gerber KK, Szpyt J, Robinson MM, Nair KS, Gygi SP, Spiegelman BM.** Detection and Quantitation of Circulating Human Irisin by Tandem Mass Spectrometry. *Cell Metab* 22: 734–740, 2015.
25. **Lara-Castro C, Fu Y, Chung BH, Garvey WT.** Adiponectin and the metabolic syndrome: mechanisms mediating risk for metabolic and cardiovascular disease. *Curr Opin Lipidol* 18: 263–270, 2007.
26. **Lee P, Linderman JD, Smith S, Brychta RJ, Wang J, Idelson C, Perron RM, Werner CD, Phan GQ, Kammula US, Kebebew E, Pacak K, Chen KY, Celi FS.** Irisin and FGF21 are cold-induced endocrine activators of brown fat function in humans. *Cell Metab* 19: 302–309, 2014.
27. **Li X, Liu J, Wang G, Yu J, Sheng Y, Wang C, Lv Y, Lv S, Qi H, Di W, Yin C, Ding G.** Determination of UCP1 expression in subcutaneous and perirenal adipose tissues of patients with hypertension. *Endocrine* 50: 413–423, 2015.
28. **Nagai N, Sakane N, Tsuzaki K, Moritani T.** UCP1 genetic polymorphism (−3826 A/G) diminishes resting energy expenditure and thermoregulatory sympathetic nervous system activity in young females. *Int J Obes* 35: 1050–1055, 2011.
29. **Nagano G, Ohno H, Oki K, Kobuke K, Shiwa T, Yoneda M, Kohno N.** Activation of classical brown adipocytes in the adult human perirenal

depot is highly correlated with PRDM16-EHMT1 complex expression. *PLoS One* 10: e0122584, 2015.
30. **Nicholls DG, Bernson VS, Heaton GM.** The identification of the component in the inner membrane of brown adipose tissue mitochondria responsible for regulating energy dissipation. *Experientia Suppl* 32: 89–93, 1978.
31. **Polyzos SA, Mathew H, Mantzoros CS.** Irisin: A true, circulating hormone. *Metabolism* 64: 1611–1618, 2015.
32. **Puigserver P, Wu Z, Park CW, Graves R, Wright M, Spiegelman BM.** A cold-inducible coactivator of nuclear receptors linked to adaptive thermogenesis. *Cell* 92: 829–839, 1998.
33. **Rabiee F, Forouzanfar M, Ghazvini Zadegan F, Tanhaei S, Ghaedi K, Motovali Bashi M, Baharvand H, Nasr-Esfahani MH.** Induced expression of Fndc5 significantly increased cardiomyocyte differentiation rate of mouse embryonic stem cells. *Gene* 551: 127–137, 2014.
34. **Ramirez-Zacarias JL, Castro-Munozledo F, Kuri-Harcuch W.** Quantitation of adipose conversion and triglycerides by staining intracytoplasmic lipids with Oil red O. *Histochemistry* 97: 493–497, 1992.
35. **Raschke S, Elsen M, Gassenhuber H, Sommerfeld M, Schwahn U, Brockmann B, Jung R, Wisloff U, Tjonna AE, Raastad T, Hallen J, Norheim F, Drevon CA, Romacho T, Eckardt K, Eckel J.** Evidence against a beneficial effect of irisin in humans. *PLoS One* 8: e73680, 2013.
36. **Roca-Rivada A, Castelao C, Senin LL, Landrove MO, Baltar J, Belen Crujeiras A, Seoane LM, Casanueva FF, Pardo M.** FNDC5/irisin is not only a myokine but also an adipokine. *PLoS One* 8: e60563, 2013.
37. **Rodríguez A, Becerril S, Méndez-Giménez L, Ramírez B, Sáinz N, Catalán V, Gómez-Ambrosi J, Frühbeck G.** Leptin administration activates irisin-induced myogenesis via nitric oxide-dependent mechanisms, but reduces its effect on subcutaneous fat browning in mice. *Int J Obes (Lond)* 39: 397–407, 2015.
38. **Sidossis L, Kajimura S.** Brown and beige fat in humans: thermogenic adipocytes that control energy and glucose homeostasis. *J Clin Invest* 125: 478–486, 2015.
39. **Spiegelman BM.** Banting Lecture 2012: Regulation of adipogenesis: toward new therapeutics for metabolic disease. *Diabetes* 62: 1774–1782, 2013.
40. **Sun W, Wang H, Li Y, Zhou X, Teng Y, Chen J.** Acquisition of pig intramuscular preadipocytes through dedifferentiation of mature adipocytes and establishment of optimal induction conditions. *Genet Mol Res* 12: 5926–5936, 2013.
41. **Svensson PA, Lindberg K, Hoffmann JM, Taube M, Pereira MJ, Mohsen-Kanson T, Hafner AL, Rizell M, Palming J, Dani C, Svensson MK.** Characterization of brown adipose tissue in the human perirenal depot. *Obesity (Silver Spring)* 22: 1830–1837, 2014.
42. **Valve R, Heikkinen S, Rissanen A, Laakso M, Uusitupa M.** Synergistic effect of polymorphisms in uncoupling protein 1 and beta3-adrenergic receptor genes on basal metabolic rate in obese Finns. *Diabetologia* 41: 357–361, 1998.
43. **Vosselman MJ, Hoeks J, Brans B, Pallubinsky H, Nascimento EB, van der Lans AA, Broeders EP, Mottaghy FM, Schrauwen P, van Marken Lichtenbelt WD.** Low brown adipose tissue activity in endurance-trained compared with lean sedentary men. *Int J Obes (Lond)* 39: 1696–1702, 2015.
44. **Wrighton KH, Lin X, Feng XH.** Critical regulation of TGFbeta signaling by Hsp90. *Proc Natl Acad Sci USA* 105: 9244–9249, 2008.
45. **Wu J, Bostrom P, Sparks LM, Ye L, Choi JH, Giang AH, Khandekar M, Virtanen KA, Nuutila P, Schaart G, Huang K, Tu H, van Marken Lichtenbelt WD, Hoeks J, Enerback S, Schrauwen P, Spiegelman BM.** Beige adipocytes are a distinct type of thermogenic fat cell in mouse and human. *Cell* 150: 366–376, 2012.
46. **Xie C, Zhang Y, Tran TD, Wang H, Li S, George EV, Zhuang H, Zhang P, Kandel A, Lai Y, Tang D, Reeves WH, Cheng H, Ding Y, Yang LJ.** Irisin Controls Growth, Intracellular Ca2+ Signals, and Mitochondrial Thermogenesis in Cardiomyoblasts. *PLoS One* 10: e0136816, 2015.
47. **Xiong XQ, Chen D, Sun HJ, Ding L, Wang JJ, Chen Q, Li YH, Zhou YB, Han Y, Zhang F, Gao XY, Kang YM, Zhu GQ.** FNDC5 overexpression and irisin ameliorate glucose/lipid metabolic derangements and enhance lipolysis in obesity. *Biochim Biophys Acta* 1852: 1867–1875, 2015.
48. **Yoon JC, Chickering TW, Rosen ED, Dussault B, Qin Y, Soukas A, Friedman JM, Holmes WE, Spiegelman BM.** Peroxisome proliferator-activated receptor gamma target gene encoding a novel angiopoietin-related protein associated with adipose differentiation. *Mol Cell Biol* 20: 5343–5349, 2000.
49. **Zhang Y, Li R, Meng Y, Li S, Donelan W, Zhao Y, Qi L, Zhang M, Wang X, Cui T, Yang LJ, Tang D.** Irisin stimulates browning of white adipocytes through mitogen-activated protein kinase p38 MAP kinase and ERK MAP kinase signaling. *Diabetes* 63: 514–525, 2014.